

**REEF ACCRETION DURING THE LAST 700 YEARS
IN THE OUTER INSULAR SHELF OF
SOUTHWEST PUERTO RICO**

by

Marianela Mercado Burgos

A thesis submitted in partial fulfillment of the requirements for the degree of

MASTER OF SCIENCE

in

GEOLOGY

UNIVERSITY OF PUERTO RICO

MAYAGÜEZ CAMPUS

2012

Approved by:

Hernán Santos Mercado, Ph.D.
Member, Graduate Committee

Date

Clark Sherman, Ph.D.
Member, Graduate Committee

Date

Wilson R. Ramírez Martínez, Ph.D.
President, Graduate Committee

Date

Julio Morell Rodríguez, M.S.
Representative of Graduate Studies

Date

Lizzette A. Rodríguez Iglesias, Ph.D.
Chairperson of the Department

Date

Abstract

Previous studies reported ceased accretion for shelf edge reefs in southwest Puerto Rico after 6,000 yrs. Four cores were recovered from spur and groove reefs, on the outer shelf; to characterize changes in the reef stratigraphy and structure that could document reasons for changes in reef accretion. Three major constituents were found: *Montastrea annularis* complex (*M. annularis*, *M. faveolata*, *M. franksi*) coral fragments, *Acropora palmata* coral fragments and coral rubble. Total recovery from these reefs show most of the content composed of coral fragments (48%), followed by coral rubble (33%), in situ corals (17%) and crustose coralline algae (2%); being in situ corals relatively uncommon in the geologic record. The major reef builder is corals of the Mn complex while recoveries of *A. palmata* specimens were mostly in the form of fragments and not in place. Analyses of bioerosion processes documented removal of coral material mainly by *Lithophaga sp.*, sponges and serpulid worms, responsible for up to 80% of microborings and 65% of macroborings. Recent radiocarbon ages ($70 - 680 \pm 25$ yrs) in these corals show accretion rates ranging from 1.1 to 3.4 m/1,000 yrs in three of the four cores representing average values according to the literature. Average accretion rate is 2.3 m/1,000 yrs. The topography seen today of the spurs studied could have started about 1,000 to 2,000 years ago. The spur and groove "recent" Holocene reef sequence obtained in southwest Puerto Rico shows the natural variability of reef materials deposition and accretion. The new data documents recent reef accretion and bring important information about the platform development and history which was unknown until now.

Resumen

Estudios pasados reportaron un cese en acreción en el veril de la plataforma insular hace 6,000 años en el suroeste de Puerto Rico. Se extrajeron cuatro barrenos de los arrecifes de surcos y estribos, cercanos al veril, para caracterizar los cambios en estratigrafía y estructura que pudiera indicar cambios en acreción. Se encontraron tres componentes principales: corales del complejo *Montastrea*, *Acropora palmata* y detritos de coral. El contenido de estos barrenos muestra que hay una abundancia mayor de fragmentos de coral (48%), seguido por detritos de coral (33%), corales en posición de crecimiento (17%) y algas coralinas encrustadoras (2%), siendo los corales en posición de crecimiento menos abundantes en el record geológico. El componente que más contribuye a la construcción del arrecife son los corales del complejo *Montastrea* mientras que el contenido recuperado de *A. palmata* son considerados fragmentos transportados. Análisis de procesos de bioerosión indican que la remoción del material coralino es mayormente causada por *Lithophaga sp.*, esponjas perforadoras y serpúlidos, responsables de hasta 80% de la micro-bioerosión y 65% de la macro-bioerosión. Datos de análisis de carbono¹⁴ en estos corales indican edades recientes ($70-680 \pm 25$ años) y muestran tasa de acreción de 1.1 a 3.4 m/1,000 años, siendo el promedio 2.3 m/1,000 años. Estos valores son similares a los publicados previamente en la literatura científica. La morfología que se observa en el presente en estos arrecifes pudo haberse originado algunos 1,000 a 2,000 años atrás. Los resultados obtenidos en los arrecifes de surcos y estribos del Holoceno muestran la variabilidad natural en acreción. Estos datos documentan acreción reciente y brindan información nueva e importante sobre el desarrollo e historia de la plataforma que se desconocía.

To my family...

ACKNOWLEDGEMENTS

During the development of my graduate studies in the University of Puerto Rico several persons and institutions collaborated directly and indirectly with my research. Without their support it would be impossible for me to finish my work. That is why I wish to dedicate this section to recognize their support.

I want to start expressing a sincere acknowledgement to my advisor, Dr. Wilson Ramirez because he gave me the opportunity to research under his guidance and supervision. I received motivation, encouragement, confidence and support from him during all my studies. I also want to thank the motivation, inspiration and support I received from Mr. Danny Harrelson from the Engineer Research and Development Center-USACE.

To the Puerto Rico Seismic Network which provided the funding for my studies and where I learned invaluable skills and knowledge to face many of the challenges of science, as well as emergency response, teamwork, discipline and responsibility.

To my very special friend Mónica Santiago Gordián for everything!, because her help has been unique; and last but the most important, I would like to thank my family: Luis Alberto Mercado Molina, Nydia Esther Burgos Loyo, Nilmaries Mercado Burgos, Meralys Mercado Burgos, Amaya Martínez Mercado, for their unconditional support, inspiration, love and because they always trust in me.

This research was supported by University of Puerto Rico Sea Grant College Program Project No. R-111-1-08 to C. Sherman and W. Ramírez.

Table of Contents

ABSTRACT	II
RESUMEN	III
ACKNOWLEDGEMENTS	V
TABLE OF CONTENTS	VI
TABLE LIST	VIII
FIGURE LIST	IX
1 INTRODUCTION.....	1
1.1 GENERAL INTRODUCTION.....	1
1.2 MOTIVATION.....	1
1.3 OBJECTIVES.....	3
1.4 LITERATURE REVIEW.....	3
1.4.1 <i>PARGUERA REEF HISTORY</i>	3
1.5 REEF ACCRETION.....	6
1.6 REEF BUILDERS.....	8
1.7 STUDY AREA	9
2 METHODOLOGY.....	11
2.1 DIVING RECONNAISSANCE.....	11
2.2 EQUIPMENT	12
2.3 CORE DESCRIPTIONS.....	13
2.4 THIN SECTION ANALYSIS	14
2.5 RADIOCARBON DATES	15
2.6 STRATIGRAPHIC COLUMNS	16
3 RESULTS AND DISCUSSION	17
3.1 STRATIGRAPHY	17
3.1.1 CORES COMPONENTS DESCRIPTIONS.....	17
3.1.2 CORES SEDIMENTOLOGIC DESCRIPTIONS	30
3.1.3 CORES BIOEROSION DESCRIPTIONS	36
3.2 ACCRETION RATES	47
3.3 ACCRETION RATES IN THE CARIBBEAN.....	51
3.4 INTERPRETATION.....	52
4 CONCLUSIONS	56
5 FUTURE WORK	57
APPENDIX A. CORES DETAILED DESCRIPTIONS	58
REFERENCES	66

Table List

Tables	Page
TABLE 2.1 Cores location and depth.....	12
TABLE 2.2 Calibrated radiocarbon ages for five corals from three cores (Clark Sherman, unpub.).....	15
TABLE 3.2 Accretion rates calculated from radiocarbon ages from corals located at different intervals along the cores.....	48
TABLE 3.3 Reef accretion rates in different Caribbean reefs.....	51

Figure List

Figures	Page
Figure 1.1: Sea level curve changes during the last 18,000 years. Modified from Macintyre, 2007.....	4
Figure 1.2: Calibrated time-depth plot for Caribbean <i>A. palmata</i> (solid line). Lightly et al. (1982) sea level curve (dashed line). Modified from Macintyre, 2003.....	4
Figure 1.3: History of coral reef accretion at Parguera shelf. Modified from Hubbard et al. (2008).....	6
Figure 1.4: Location of sampling sites on southwest insular shelf (NOAA/PRSN).....	10
Figure 2.1: Spurs (reefs) located close to the shelf edge (photo: Clark Sherman).....	11
Figure 2.2: <i>A. palmata</i> colony found in place at the top of the spurs (photo: Clark Sherman).....	12
Figure 2.3: Clark Sherman and Milton Carlo coring on top of a spur in the outer shelf.....	13
Figure 3.1: LP-1 core content showing Mn Complex coral as the dominant specie (76%) and also as a reef builder (18%).....	20
Figure 3.2: Crustose coralline red algae on the stratigraphic top of the core.....	21
Figure 3.3: Corallite of Mn complex showing its 24 septa (core depth: 120 cm).....	22
Figure 3.4: LP-2 core has the highest amount (13%) of <i>A. palmata</i> fragments found.....	23
Figure 3.5: A section containing Mn complex on top, <i>A. palmata</i> below and Mn complex coral fragments at the bottom (core depth: 0-4 cm).....	24
Figure 3.6: <i>A. palmata</i> fragment (above) encrusted by crustose coralline algae (below) (core interval 25-60 cm). Mn complex fragment is located just below the coralline algae.....	24
Figure 3.7: LP-3 core content where the highest percentage (68%) of coral rubble was recovered.....	25
Figure 3.8: Coral rubble in 28-74 cm core interval.....	26
Figure 3.9: <i>Colpophyllia sp.</i> fragment identified at core depth: 55 cm.....	26
Figure 3.10: Crustose coralline algae laminations and encrusting forams alternations at the top of the core.....	26
Figure 3.11: LP-3A core content where the highest recovery (85%) of Mn Complex and framework was obtained.....	28
Figure 3.12: <i>A. palmata</i> found at the stratigraphic top of LP-3A core.....	29
Figure 3.13: Corallite of a Mn complex (core depth: 130-135 cm).....	29
Figure 3.14: Acicular cement in Mn Complex coral fragment (core depth: 130-135 cm).....	29
Figure 3.15: A piece of coral rubble with borings filled with mud (core interval: 0-20 cm).....	31
Figure 3.16: Mud and peloids in a Mn Complex coral fragment (core depth: 120 cm).....	31
Figure 3.17: Crustose coralline algae located on top of the <i>A. palmata</i> fragment (top of the core).....	31
Figure 3.18: At the center right of the photo sand sized sediments are visible.....	32
Figure 3.19: Sediments inside internal structure of an <i>A. palmata</i> coral fragment (core depth:79-87 cm).....	33
Figure 3.20: Horizontally oriented geopetals in <i>A. palmata</i> fragment at core depth: 79-87 cm.....	33

Figure 3.21: Inverted geopetals in <i>A. palmata</i> fragment at core interval: 25-60 cm.....	33
Figure 3.22: Sand-sized sediments located in a Mn complex fragment (core depth: 10 cm).....	34
Figure 3.23: Clasts (mostly skeletal fragments) deposited in a boring at the top of the core (0-3 cm).....	34
Figure 3.24: Sand in <i>A. palmata</i> internal structure at the top of the core.....	35
Figure 3.25: Mud in boring includes some benthic forams (core depth: 135 cm).....	35
Figure 3.26: Borings as geopetals (1 mm to 5 cm) at Mn complex fragment in LP-3A (core interval 70-114 cm).....	36
Figure 3.27: A piece of coral rubble at LP-1 with many (more than 40) small borings (1 mm and less) (core interval: 20-25 cm).....	38
Figure 3.28: Macroboring (black bars) and microboring (gray bars) percentage in LP-1 content.....	39
Figure 3.29: Macroboring (black bars) and microboring (gray bars) percentage in LP-2 content.....	41
Figure 3.30: Borings (1 mm to 1.8 cm), some created by <i>Lithophaga sp.</i> in <i>A. palmata</i> coral fragment at 60-103 cm core interval.....	42
Figure 3.31: Mn complex coral fragment with abundant borings (stratigraphic top of the core located at the surface of the reef).....	43
Figure 3.32: Coral rubble fragments with abundant borings (core interval: 0-28 cm).....	43
Figure 3.33: Macroboring (black bars) and microboring (gray bars) percentage in LP-3 content.....	44
Figure 3.34: <i>Lithophaga sp.</i> located in boring (1 mm to 2.5 cm) while other borings are visible around (core LP-3A interval: 36-70 cm).....	45
Figure 3.35: Macroboring (black bars) and microboring (gray bars) percentage in LP-3A content.....	46
Figure 3.36: Serpulid tube located in <i>A. palmata</i> coral fragment at the top of the core.....	47
Figure 3.37: Stratigraphic columns of the cores showing the accretion rates in m/1,000 years.....	49
Figure 3.38: Stratigraphic correlation using radiocarbon ages (260 to 320 ± 25 ybp) in three cores.....	50
Figure 3.39: Reef diagram showing possible area were rubble can accumulate. Modified from Scoffin, 1987.....	53

1 INTRODUCTION

1.1 General Introduction

Coral reefs are important marine ecosystems where many biological, chemical and physical processes interplay. They support thousands of species and communities per unit area, much more than any other marine environment. Also they have economic value since they are areas of natural beauty for recreation, sources of food, jobs, chemicals, pharmaceuticals and shoreline protection. They are important producers of carbonate sediments and are found in many tropical zones. The differences in their structure and morphology may respond to previous bottom topography, faunal interactions and physical processes like terrigenous sedimentation or proximity to shore (Darwin, 1842; Hubbard et al., 1997; Morelock et al., 2001). Physical, chemical, and biological processes also cause variations in different aspects of the reef system on both spatial and temporal scales. The biological structures and reef morphology can be recognizable in the ancient record. Both criteria along with other analyses are important to understand the environment and conditions in which these ecosystems thrive.

1.2 Motivation

Reefs around the world have experienced dramatic changes that have been attributed to diseases, pollution, global climate change and many others. Investigations have shown that reefs are in a critical health state (Hughes et al., 2003) and the cause seems to be in part anthropogenic (Mora, 2008), (Pandolfi et al., 2003), (Ryan et al., 2008). Debates on what is causing coral reefs

around the world to be threatened are complex and a way to gather data relevant for the debate is to look at the fossil record.

Surveys of the modern reefs in southwest Puerto Rico (Morelock et al., 2001) documented large areas of dead reef surfaces composed of in situ dead coral rock covered by algal-sediment mats. The presence of these dead reef surfaces indicates that environmental conditions once existed in these areas that were conducive to coral growth, but then conditions changed causing mortality and a significant decrease of active coral cover and growth. Morelock et al. (2001) proposed that much of the benthic habitat of the insular shelf of southwest Puerto Rico has changed from live coral reef to “hard ground” with little or no live coral cover. Evidence suggests that some of this change has been caused by human activities negatively affecting the coastal environment. However, natural variability in the reef system could also be responsible of some of the changes in coral distribution and cover.

Studies of Pleistocene reefs have shown high variability in the character of reefs at fine spatial and temporal scales (Pandolfi and Jackson, 1997). Similarly, accretion of *A. palmata* reefs located at the shelf edge in La Parguera, PR, has been shown to stopped ~6,000 years ago, in relation to long term changes in the shelf environment (Hubbard et al., 1997, Morelock et al., 2001). Not only *A. palmata* reefs vanished around 6,000 ybp, they later showed an apparent recover until about 3,000 ybp, when stopped accreting again letting no evidence in the geologic record of reappearance as a reef builder in the outer shelf (Hubbard et al., 1997).

Holocene reefs in the insular southwest shelf of Puerto Rico contain an important archive of reef decline and re-colonization that may indicate changing environmental conditions. This investigation has documented changes in reef accretion during the last 700 years and proposed

possible explanations. The geologic history of these Holocene reefs may provide important information on the magnitude of natural variability from the perspective of accretion.

1.3 Objectives

The primary objective of this study is to find variations in the reef structure that could be associated with differences in accretion during the last 700 years. Efforts were focused on studying the stratigraphy and sedimentology of the upper two meters of the reef structures on the outer insular shelf off Parguera, southwest Puerto Rico. Using these data is possible to detect changes in the reef structure and composition during the last 700 years. Understanding these recent changes in the reef structure, composition, and accretion will allow us to understand the dynamics and variability of the reef system in southwest Puerto Rico.

1.4 Literature Review

1.4.1 *Parguera Reef History*

During the last 18,000 years the world has experienced a eustatic sea level rise of about 100 m as consequence of late Pleistocene ice sheets melting. The last 10,000 years have been significantly important in terms of sea level due to a change in climatic conditions from a relatively cooler environment in the Pleistocene to a dramatic warm epoch during the Holocene. Coral reefs of the western Atlantic have experienced extreme changes due to this Holocene Transgression (Macintyre, 2007) (Fig. 1.1). During the last two thousand years sea level has raised about two meters (see red box in Fig. 1.2).

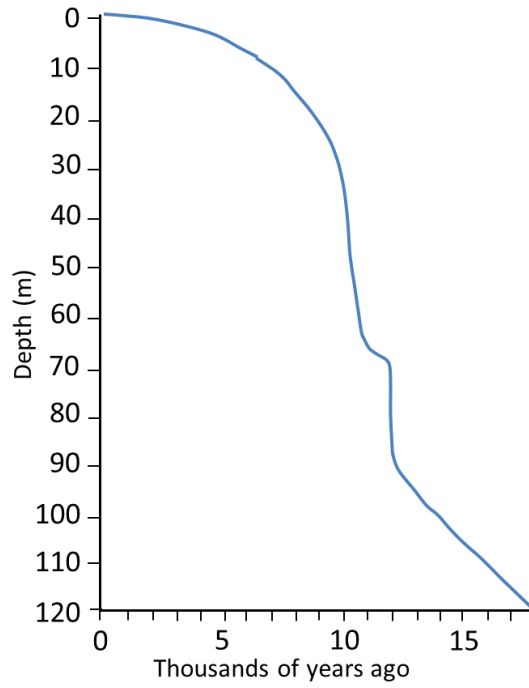


Figure 1.1. Sea level curve changes during the last 18,000 years. Modified from Macintyre, 2007.

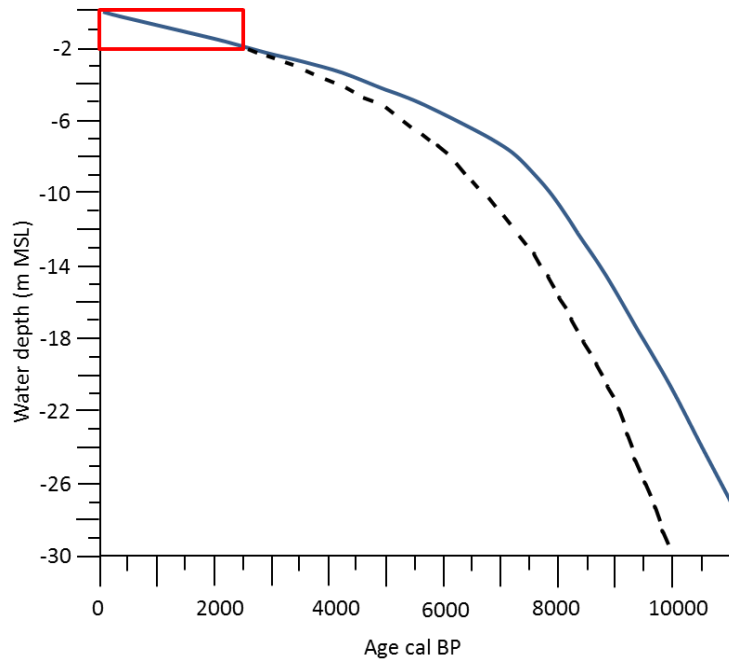


Figure 1.2. Calibrated time-depth plot for Caribbean *A. palmata* (solid line). Lightly et al. (1982) sea level curve (dashed line). Modified from Toscano and Macintyre, 2003.

Holocene reefs in Parguera formed over an antecedent Pleistocene topography about 10,000 ybp, some 13-23 m below present sea level. Until 6,000 ybp these reefs were keeping up with sea level (Fig. 1.3). Around 6,000 ybp a backstepping of some 6 km occurred moving from *A. palmata* reefs in the shelf edge to massive species reefs in shallower waters. This is reported in the geologic record as a gap in *A. palmata* vertical accretion on the outer shelf. Much later new *A. palmata* reefs colonized on top of previous reef surface dominated by more sediment tolerant species like *MaC* species which were present inland. This shift in species has been interpreted as the corals response to higher terrigenous sedimentation coming from inland. Another gap in *A. palmata* reefs has been documented at about 3,000 ybp (inner reefs). At the Parguera shelf edge the *A. palmata* reefs stopped accreting at about 6,000 ybp according to Hubbard et al. (1997). This is represented as a relict reef in figure 1.3. The possible causes for the phenomenon presented by Hubbard et al. (1997) are the presence of more sediment tolerant corals in landward areas, sudden changes in larval supply, changes in hydrologic conditions favoring sediment tolerant species and/or climatologically causes altering water conditions into turbid environments due to input of terrestrial sediments.

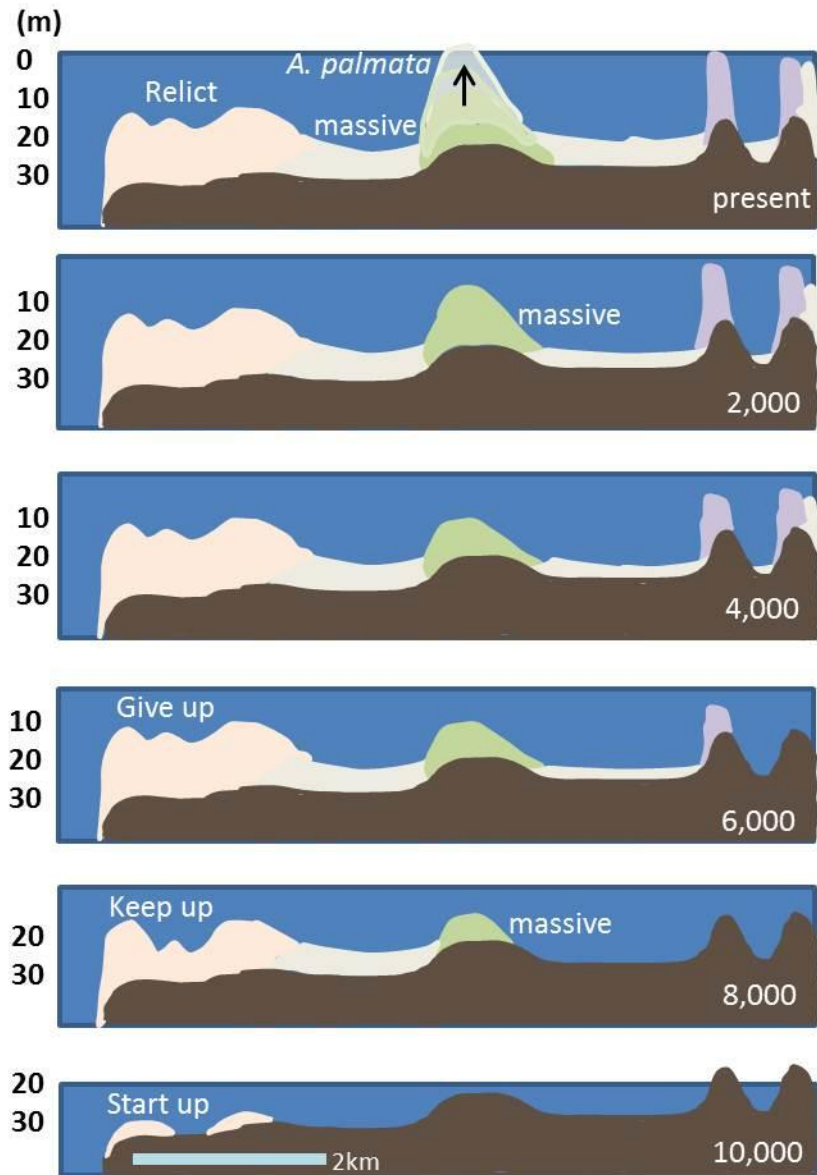


Figure 1.3. History of coral reef accretion at Parguera shelf. Modified from Hubbard et al., 1997.

1.5 Reef accretion

“A reef is a laterally restricted mass of carbonate rock whose composition and relationship with the surrounding sediments suggest that the bulk of its components, normally skeletons, were bound together into a framework during deposition, maintaining and developing a structure of

positive topographic relief on the sea-bed” (Scoffin, 1987). The ability of a reef in maintaining its structure and to accomplish its geomorphic function is greatly influenced by net rates of carbonate production and accumulation (Perry and Hepburn, 2008). A series of processes including physical, chemical and biological interactions help to cycle the calcium carbonate in reef environments. These processes not only work at the scale of individual colony, corals as an example, but they can combine and influence the overall reef accretion, in some cases allowing the development of a reef; while in others results in the removal of the carbonate framework. Once the sediment is produced it can follow incorporation into reef framework, be exported out of the reef or be deposited within other depositional settings (Perry and Hepburn, 2008). These processes of cycling the carbonate produced may exert a ‘constructive’ or ‘destructive’ control (Scoffin, 1992). This in turn can influence the carbonate production in the reef (Perry and Hepburn, 2008) and also determine the rates of net calcium carbonate accumulation. These processes may work in different timescales and can also vary spatially. Corals, being one of the primary elements, add vast quantities of carbonate per area and are a constructive component in a reef (Vecsei, 2004). But corals are not alone in the primary production of carbonate; other important calcium carbonate producers are calcareous encrusters, particularly the crustose coralline algae and the precipitation of cements (Perry and Hepburn, 2008). Given that corals and crustose coralline algae contribute large amounts of carbonate into the reef structure they commonly dominate the calcium carbonate accumulation in specific reef settings (Steneck and Adey, 1976; Hallock and Schlager, 1986). Considering the ‘destructive’ side, many biological and physical processes determine the rates of net calcium carbonate accumulation, for example bioerosion. This important process is caused by a variety of marine organisms including some fishes, echinoids, endolithic cyanobacterias, chlorophytes, fungi, sponges, bivalves and worms

(Bak, 1994; Bruggeman et al., 1996; Scaps and Dennis, 2008; Perry and Hepburn, 2008). This fauna play main roles within the reefs. First, they can directly degrade the primary and secondary framework increasing the susceptibility to erosion by physical and chemical processes, and influencing the carbonate budgets (Goreau and Hartman, 1963; Frydl and Stearn, 1978; Bak 1994). Second, they can produce significant amounts of sediment (Neumann, 1966; Gygi 1975; Moore and Shedd, 1977). Reef framework development can be affected by physical disturbances like storms and cyclones which generate coral rubble (Hubbard et al., 1997; Rasser and Riegl 2002; Blanchon et al., 1997). All these processes are crucial to the reef building potential, defined by the carbonate budget, an approach to quantify reef production performance. A carbonate budget considers the gross carbonate production from corals and calcareous encrusters, and also the sediment produced or imported into the reef, subtracting the sediment lost through erosion by biological and physical agents, dissolution or sediment exportation (Chave et al. 1972). Scoffin (1992) terms were used being ‘primary’, the corals and ‘secondary’, the calcareous encruster, as carbonate producers, and also the destructive group named bioeroders. Basically these three biogenic groups are responsible for the net rates of carbonate accumulation in a particular reef and also are the most directly affected by environmental and ecological changes (Perry and Hepburn, 2008).

1.6 Reef builders

The main reef builders are corals which are responsible in constructing the framework. The *Montastrea annularis complex* is referred to the species *Montastrea annularis*, *Montastrea faveolata* and *Montastrea franksi* (Knowlton et al., 1997) and will be referred here as *M. annularis complex*. These name species still remain inconclusive (Szmant et al., 1997) and some

have not accepted (Van Veghel and Bak, 1993), since there is much overlap in characteristics and there are no diagnostic genetic differences among them. The *M. annularis* complex species have been extensively documented as a reef builder in the Caribbean (Van Veghel and Bak, 1993; Carricart-Ganivet, 2004).

1.7 Study Area

The study area is located on the insular shelf of southwest Puerto Rico, off the coast from the municipality of Lajas. The shelf varies its extension reaching up to approximately 11 km in some areas before the abrupt drop that goes into the Caribbean Sea depths.

The platform was subdivided in inner, middle and outer shelf. The inner shelf is shallow with approximately depth of 3-4 meters with reef shoals and reef flats present. The mid-shelf reefs are between 2-4 km from the shore at depths of 14-16 m. At the shelf edge reefs are at depths ranging from 13 m to over 35 m. In general the typical reef zonation for the Caribbean is present with slight variations. Head corals like *M. annularis* complex and the branching coral *Acropora cervicornis* are present from 10 to 20 m depth. The branching *A. palmata* is present in shallower waters (Hubbard et al., 1997).

Sampling sites are located some 9 kilometers south from the coast on the outer shelf. The sites were chosen based on the geomorphology of the bottom (spur and groove reefs) and previous studies (Hubbard et al. 1997) (Fig. 1.4). Four cores (1-2 m) were recovered on the outer shelf edge using a hydraulic drill (Tech 2000) property of the Department of Marine Sciences, University of Puerto Rico, Mayagüez.

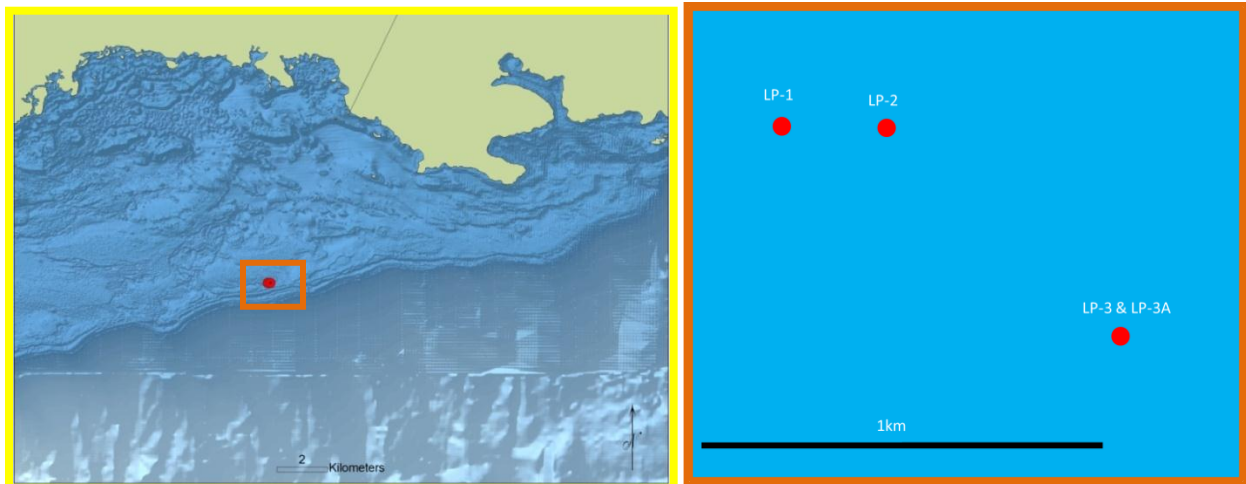
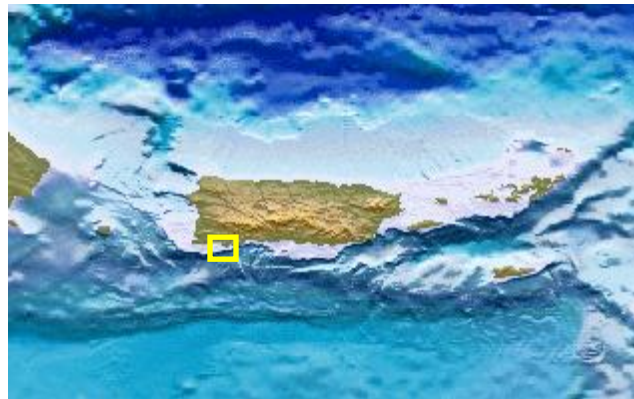


Figure 1.4. Location of sampling sites on southwest insular shelf (NOAA/PRSN).

2 METHODOLOGY

2.1 Diving reconnaissance

The presence of the coral *A. palmata* dead colonies, in growth position, at the surface of spurs located at about 60 feet deep along the outer shelf in Parguera created the motivation for this project. Diving reconnaissance was performed by Dr. Clark Sherman and other members of the diving team of the Marine Sciences Department, University of Puerto Rico at Mayagüez looking for suitable places to study the internal structure of the reef by coring. Places drilled were primarily chosen based on reef morphology (spurs and groove, fig. 2.1) because one of the cores sampled by Hubbard et al. (1997) was apparently recovered from these reefs. Also, as mentioned before, *A. palmata* dead colonies have been found in growth position at the top of these reefs (Fig. 2.2).



Figure 2.1. Spurs (reefs) located close to the shelf edge.



Figure 2.2. *A. palmata* colony found in place at the top of the spurs (photo: Clark Sherman).

2.2 Equipment

The equipment used for coring the internal structure of the reef is a diver-operated Tech 2000 submersible, hydraulic, rotary coring drill with a 7.6 cm diameter diamond-studded drill bit. A total of four cores were recovered using this equipment named LP-1, LP-2, LP-3 and LP-3A (Table 2.1). The cores were taken from spurs (reefs) located less than 1 kilometer apart to each other. All the cores were extracted at approximately 14 meters deep. Figure 2.3 shows Dr. Clark Sherman and Mr. Milton Carlo during the procedure of coring the reef.

Table 2.1. Cores location and depth.

Core name	Latitude	Longitude	Depth (m)	% Recovery
LP-1	17° 53.561'	-67° 00.611'	13.7	80
LP-2	17° 53.558'	-67° 00.596'	14	55
LP-3	17° 53.527'	-67° 00.563'	14	61
LP-3A	17° 53.527'	-67° 00.563'	14	90

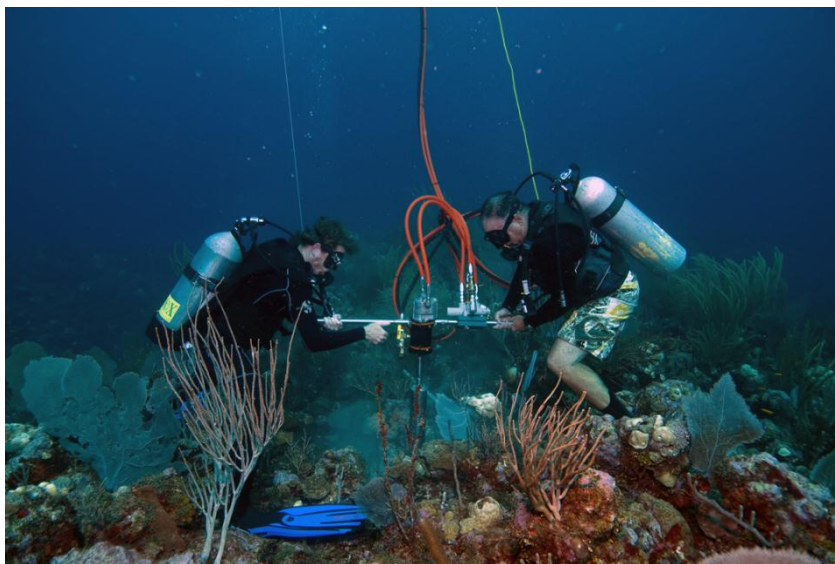


Figure 2.3. Clark Sherman and Milton Carlo coring on top of a spur reef in the outer shelf
(Photo: Héctor Ruíz, UPRM)

2.3 Core Descriptions

Once the cores were collected a description of the core components was done with naked eye and using of 10X magnification hand lenses. The total recovery of each core was quantified and differences in composition were described. Rubble pieces were counted, identified (when possible) and described. Each coral fragment (5 cm or larger) was identified using the morphologic characteristics. Coral identification guides such as NMITA (Neogene Marine Biota of Tropical America) and Paul Humann and DeLoach (1992) were used. The latter was also useful to identify organisms and fragments of them. Careful analyses of each sample was also performed using hand-lenses to identify other smaller organisms and organism structures like borings and other structures associated with the reef processes.

Bioerosion percentage was calculated for hand samples (macroborings) and thin section samples (microborings) using point counting method (150 points) of JMicrovision software. Thirteen hand samples were analyzed for macroboring percentage and fifteen thin sections for microboring percentage; all were duplicated to get precise results. Each point falling in a boring was counted no matter the times it fell in the same bored area.

2.4 Thin-section Analysis

Based on the visual analysis 20 samples were selected for thin section preparation. The selection was made primarily, for coral identification since some of the samples were difficult to identify in hand sample. In addition, thin sections were made to take a closer look at the internal structure of the coral and rubble present and to document characteristics that could be used in the interpretation of the original depositional environments from the point of view of reef zonation. The thin sections were prepared in the thin section laboratory of the Geology Department, UPRM. The procedure included to cut the samples into smaller pieces, impregnate them with epoxy in a vacuum environment, and labeling. The latter included the orientation of the pieces along the core (arrow pointing up, according to the order in which the fragment was found in the core). After two days in the oven the stubs were sliced and grinded to an appropriate thickness. Once the thin sections were prepared it was possible to identify the corals that were not easily recognized in hand-sample. The thin sections were also used to confirm the identity of the corals identified in hand sample. The number of septa was counted, the internal structures were identified using NMITA and Humann and Deloach (1992) guides. Several specimens were identified by Dr. Wilson Ramírez. Many other groups of organisms were also identified by using diagnostic features such as internal chambers in the skeletal remains, shell morphology, internal

structure, boring morphology and size. Detailed taxonomical work was not performed since it is beyond the scope of this project.

2.5 Radiocarbon Dating

Modern Scleractinian corals can be dated using radiocarbon technique. In this method, the age of the coral is obtained by analyzing the amount of ^{14}C present in the sample. Its radioactive property makes its concentrations falls and it is possible to know when it was living by using this technique. Table 2.2 shows the five coral (aragonitic) samples selected for radiocarbon technique (Clark Sherman, unpub.). These corals are located in cores and intervals: LP-1 (69-70 cm), LP-1 (146-148 cm), LP-2 (87-89 cm), LP-3A (10-11 cm) and LP-3A (110 cm). Calibrated radiocarbon ages were obtained from the National Ocean Sciences Accelerator Mass Spectrometry Facility (NOSAMS), Woods Hole Oceanographic Institution, Woods Hole, MA. Calibration of coral sample ages is important since the ocean water stores ^{14}C that could make coral samples to be older. This occurs because mixing of deep waters ($^{14}\text{CO}_2$ depleted) with shallow waters ($^{14}\text{CO}_2$ enriched) is not always homogeneous and is predominant in regions close to the equator as a consequence of trade winds (Bowman, 1990). The coral ages are important not only to know the age of the reefs cored but also to calculate accretion rates. These rates were obtained using the coral ages and the core length intervals by subtracting both parameters.

Table 2.2. Calibrated radiocarbon ages for five corals from three cores (Clark Sherman, unpub.).

Sample	Core	Depth in core (cm)
<i>M. annularis</i> complex	LP-1	69-70
<i>M. annularis</i> complex	LP-1	146-148
<i>A. palmata</i>	LP-2	87-89
<i>M. annularis</i> complex	LP-3A	10-11
<i>M. annularis</i> complex	LP-3A	110

2.6 Stratigraphic Columns

A stratigraphic column was created for each core using hand samples and thin section analysis. The scale is based on the core recovery including the corals skeletons and rubble accumulation length in the core. *M. annularis* complex coral fragments representations (dome shape) and *A. palmata* coral fragments are not intended to show corals in growth position (corallites up orientation), rather those *M. annularis* complex thought to be in situ are highlighted in yellow (see legend in page 20). Radiocarbon dates were integrated to the stratigraphic columns to compare corals age through the stratigraphic record obtained. Accretion rates were also added and are shown in units of meters per thousand years (m/ky).

3 RESULTS AND DISCUSSION

3.1 Stratigraphy

Four cores were recovered close to the shelf edge at the marine platform in southwest Puerto Rico. Recovery was different in each case, but some similarities were present. There were three major constituents in the cores: *M. annularis* complex, *A. palmata* and coral rubble. The dominant constituents were coral fragments (defined here as fragments of 5 cm in core length or larger, see legend in page 20) of the *M. annularis* complex. Some *M. annularis* complex coral colonies were drilled during the coring and represent the largest recoveries (20 to 32 cm in length each). Coral rubble was present in all the cores but its abundance varied, mostly composed of *A. cervicornis* branches. *A. palmata* coral fragments were found in all the cores but its abundance was different in each core too.

3.1.1 Cores Components Description

In the core LP-1 (17°53.561', -67°00.611' / length = 153 cm), approximately the first 60 cm of the core are mainly composed of alternating zones of coral rubble and *M. annularis* complex coral fragments. From 60 cm down to 153 cm, the core is mainly composed of *M. annularis* complex coral fragments and corals (framework), with an exception at the interval 125 to 153 cm, where coral rubble is also present (Fig. 3.1). In this core, seven zones of crustose coralline algae were found. Figure 3.2 shows an example of one of these at the top of the core. The thickness of the layers ranged from 1 to 4 mm. The greatest amount of the core material recovered was from *M. annularis* complex coral fragments with 76 %; 23% of this value suggests being in growth position (18% of total core content). To see details of *M. annularis*

complex coral fragments length refer to Appendix A. The *M. annularis* complex 24 septa corallite is shown in figure 3.3. Crustose red algae accounted for a 2% of the core content. Coral rubble accounted for 20% of total content. These highly encrusted rubble pieces varied in shapes from rounded to sub-rounded (interval 25-33 cm) and angular to subangular (interval 0-20 cm). Appendix A shows the shapes of each coral rubble zone using Power's roundness scale (1953). Few (2-3) coral rubble pieces were cemented in this core (interval: 0-20 cm), and also a coral fragment composed of *M. annularis* complex and *A. palmata* (interval: 20-25 cm) mostly aided by crustose algae, representing a 4% of this core content which has been cemented. Cement morphologies identified in this core were micritic and acicular.

Legend



Coral rubble



M. annularis complex coral fragment (5-10 cm long)



M. annularis complex coral fragment (>10-15 cm long)



M. annularis complex coral in framework (20-30 cm long)



A. palmata coral fragment



Colpophillia sp. coral fragment



Crustose coralline algae layer



Calibrated radiocarbon age



Coral and coral fragments recovery

Coral rubble recovery

No recovery

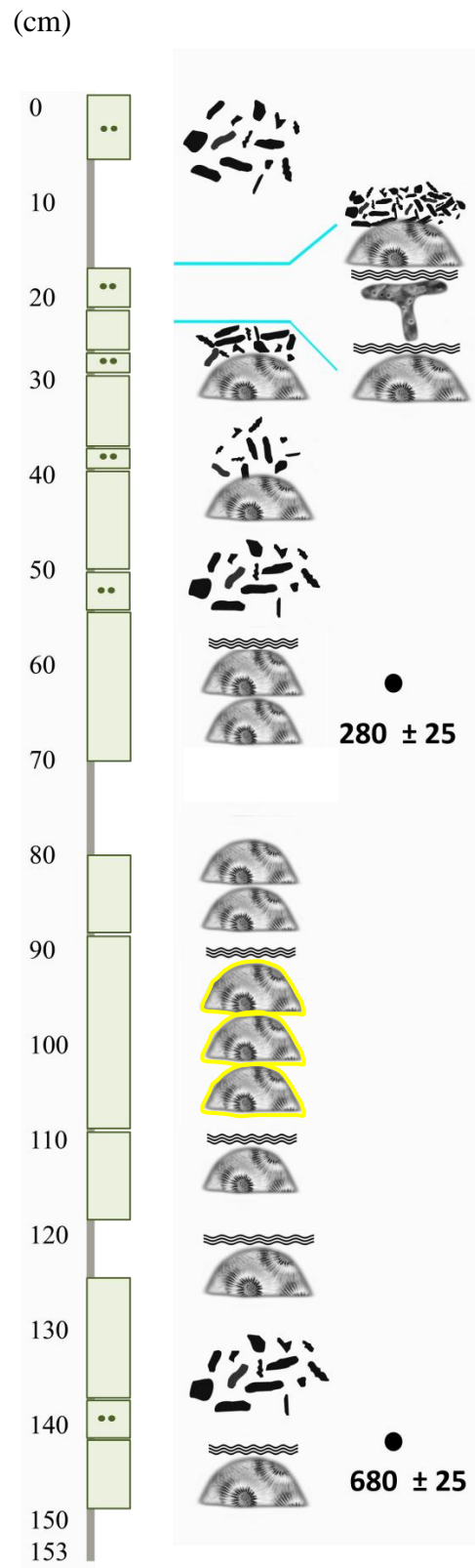


Figure 3.1. LP-1 core content showing *M. annularis* complex coral as dominant specie (76%) and also as a reef-builder (18%).

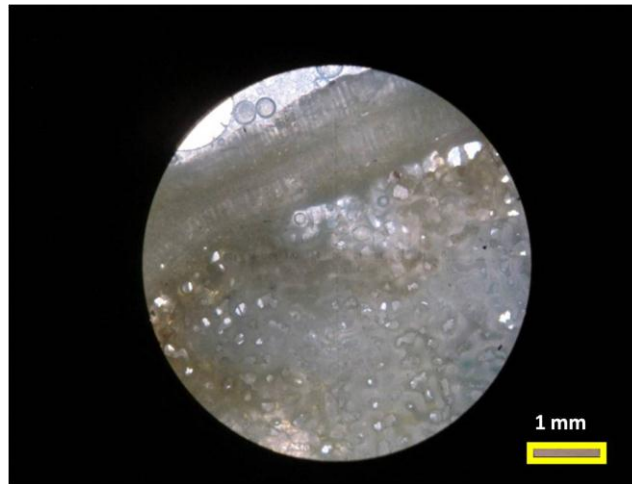


Figure 3.2. Crustose coralline red algae present on the stratigraphic top of the core.

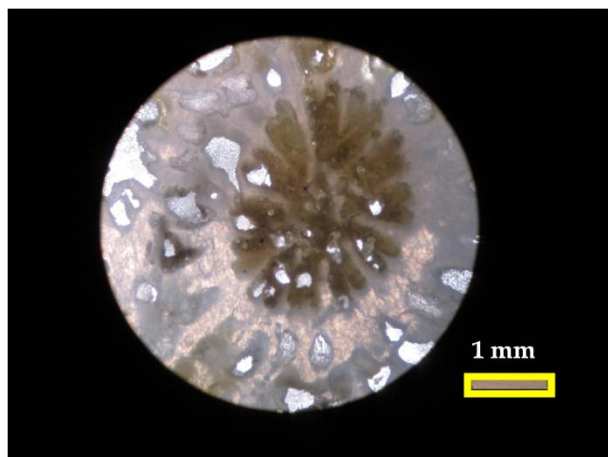


Figure 3.3. Corallite of *M. annularis* complex showing its 24 septa (core depth: 120 cm).

Core LP-2 ($17^{\circ}53.558'$, $-67^{\circ}00.596'$ / length = 172 cm), is mainly composed of coral rubble (61%) and has the greatest amount of coral rubble recovered in all the cores studied (Fig. 3.4). *A. palmata* and *M. annularis* complex coral fragments were similarly abundant in this core with 13% and 15% of the content composition respectively. Another important component was crustose red algae. Its percentage composition represents 4% of the core material. There are three core locations where a *M. annularis* complex coral fragment is cemented with an *A. palmata*

fragment; these are in core intervals: 0-25 cm; 25-60 cm and 60-103 cm. Figure 3.5 shows the first of these locations, on top of the core, from 0 to 4 cm approximately. Figures 3.6 show an example at the 25-60 cm core interval, where a layer of crustose red algae is located below the *A. palmata* fragment. Each of these three coral fragments are separated by crustose coralline algae ranging from 1 mm to 7 mm thick. A total of seven layers of crustose red algae were found through all the core content. At the last core interval (130-172 cm) the *M. annularis* complex coral fragment was only possible to identify in thin section, since in the hand sample it was not recognizable. At 140 cm coral fragments of possibly *Eusmilia sp.* and a *Colpophillia sp.* were found as part of the coral rubble pieces. Few (4-5) coral rubble pieces were cemented with other coral pieces. In addition, at 130 cm, about six *A. cervicornis* fragments were found cemented. Micritic cement was found associated with deposition in borings and inside corals internal structure. In this core, 4% of the coral fragments found have been cemented.

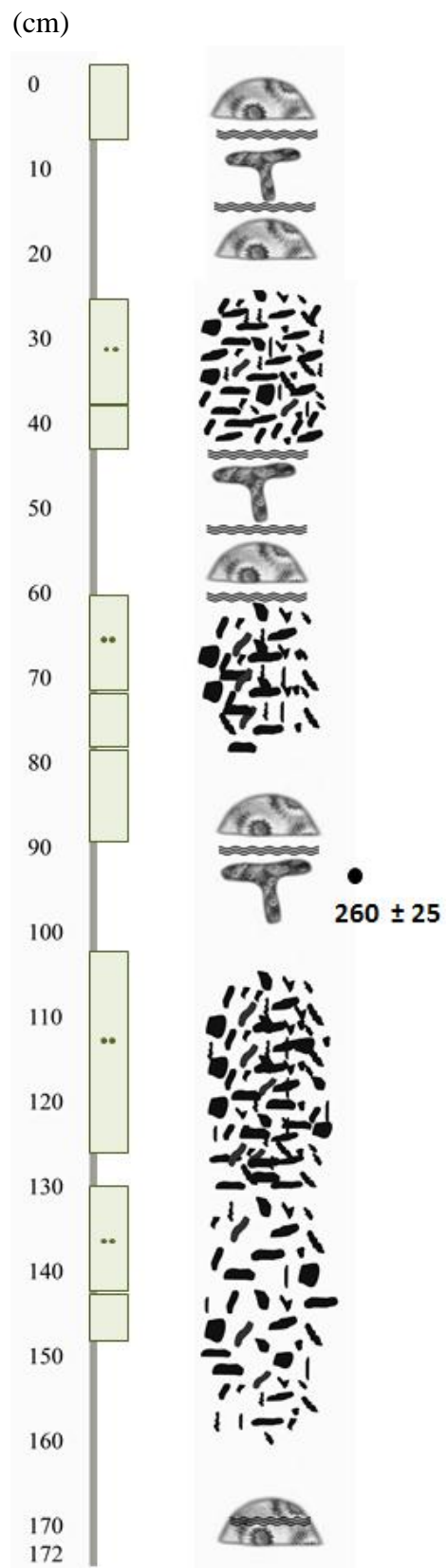


Figure 3.4. LP-2 core has the highest amount of *A. palmata* coral fragments (13%) found.



Figure 3.5. A section containing *M. annularis* complex on top, *A. palmata* below and *M. annularis* complex coral fragments at the bottom (core depth: 0 to 4 cm).

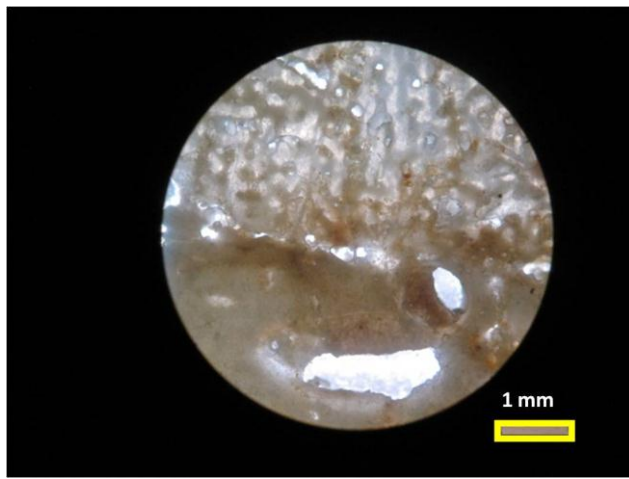


Figure 3.6. *A. palmata* fragment (above) encrusted by crustose coralline algae (below) (core interval 25-60 cm).

LP-3 is the shortest core (17°53.527', -67°00.563' / length = 74 cm). It was not possible to recover more material due to unconsolidated substratum (Clark Sherman, personal communication). The core is mainly composed of coral rubble, about 68% (Fig.3.7) and only few (2-3) pieces cemented. Figure 3.8 shows a close look of one of the pieces of rubble in thin section. *M. annularis* complex and *Colpophillia* sp. (Fig. 3.9) coral fragments abundances were similar, 10% and 13% respectively. Other important constituents were *A. palmata* fragments and crustose coralline algae with 4% and 3% respectively. The *M. annularis* complex coral fragment was found at the top of the core followed by the *A. palmata* coral fragment. The presence of *A. palmata* was identified in thin section because it was not recognizable in hand sample. A total of three zones of crustose red algae were documented ranging from 2 mm to 6 mm in thickness (Fig. 3.10).

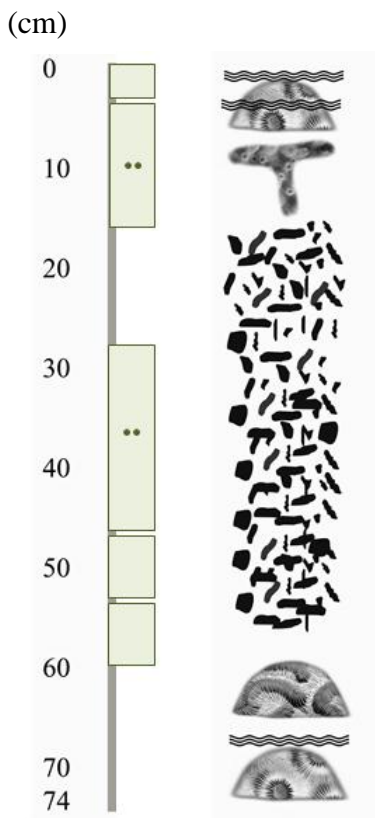


Figure 3.7. LP-3 core content where the highest percentage of coral rubble (68%) was recovered.

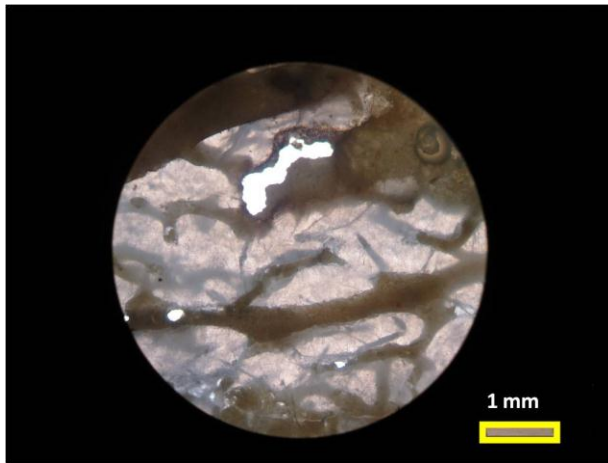


Figure 3.8. Coral rubble piece in 28-74 cm core interval.

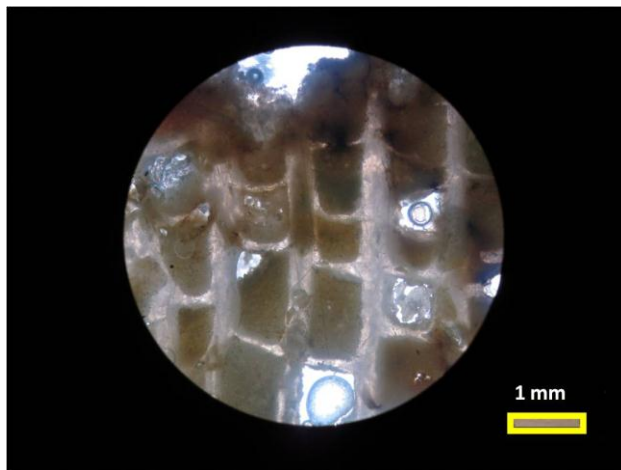


Figure 3.9. *Colpophillia* sp. fragment identified at core depth: 55 cm.

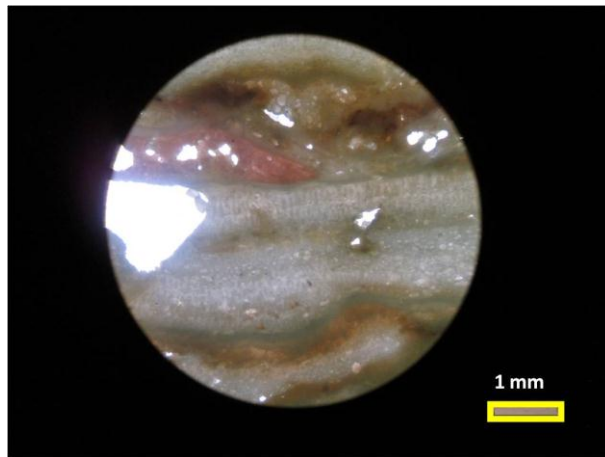


Figure 3.10. Crustose algae laminations and encrusting forams alternations at the top of the core (0 cm).

LP-3A (17°53.527', -67°00.563' / length = 136 cm) is the core with the highest recovery of *M. annularis* complex with 85% (Fig. 3.11). The *M. annularis* complex recoveries, at core depths 36 cm and 70 cm, suggest corals in growth position (corallites up orientation), representing a 50 % of total content. An *A. palmata* fragment is located at the top which represents the 5% of this specie in this core (Fig. 3.12). Two zones of coral rubble close to the bottom (110 cm and 125 cm) account for 7 % of the core content, only 2 pieces were cemented. Figure 3.13 and 3.14 show a corallite of a *M. annularis* complex found at around 130-135 cm; in the latter acicular cement has formed inside coral structure. Eight crustose red algae layers were found through this core ranging in thickness from 1 mm to 4 cm represent 1% of the content.

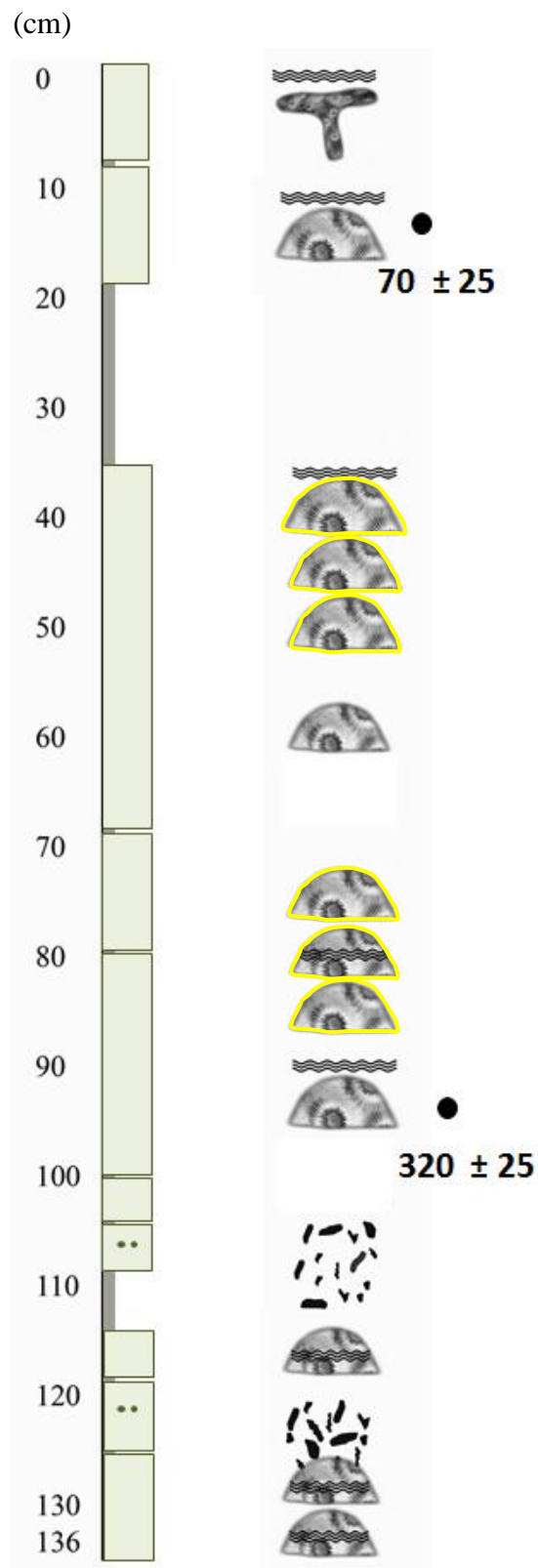


Figure 3.11. LP-3A core content where the highest recovery (85%) of *M. annularis* complex coral and 50 % of framework was obtained.

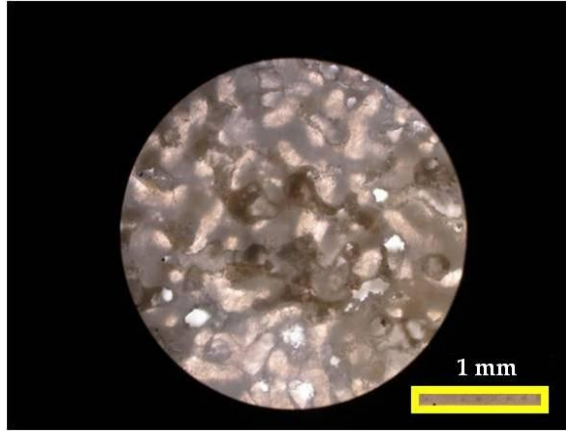


Figure 3.12. *A. palmata* found at the stratigraphic top in core LP-3A.

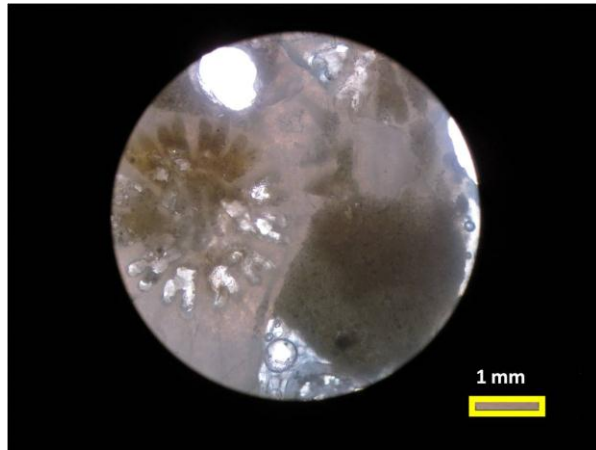


Figure 3.13. Corallite of a *M. annularis* complex (core depth: 130-135 cm).

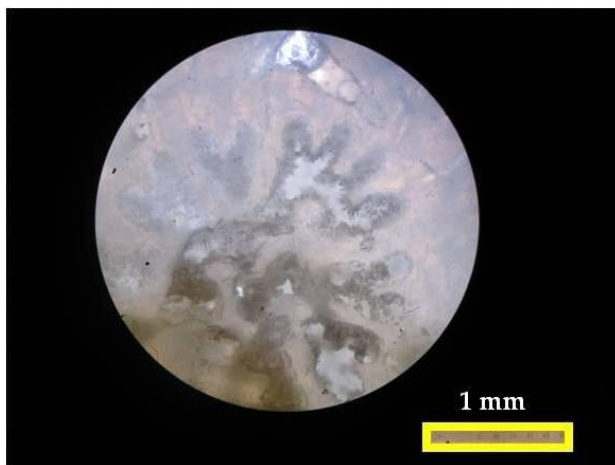


Figure 3.14. Acicular cement in *M. annularis* complex coral fragment (core depth: 130-135 cm).

3.1.2 Cores sedimentologic descriptions

The reef itself produces a lot of sediments which are incorporated and sometimes preserved in the geologic record. Corals are the main frame builders and are also hosts of transported sediments which ultimately get trapped in the internal structure of the reef. Borers, such as *Lithophaga sp.*, produce cavities where sediment can be accumulated in the internal structure of the corals. Encrusting coralline algae trap sediments making them also part of the record. These organisms contribute to the construction of the reef. Many organisms destroy the reef structure while others build it; the net result is the reef accretion which is influenced also by a variety of environmental conditions.

In the spur and groove reef cores obtained in this study, many samples showed sediments generated deposited in several ways. As an example, in LP-1, it was possible to see mud deposited in small borings of a piece of coral rubble at 0-20 cm interval (Fig. 3.15). This could suggest that the coral was attacked by borers and that after the borings were created, sediment entered, accumulated and got cemented in them. Nevertheless, it could also be micrite as a product of boring. Similarly, borings filled with sediment in the *M. annularis* complex fragment located at ~125 cm were also found. In this case, specifically peloids (0.1 – 0.3 mm) were found in the coral internal structure facilitated by borings (Fig. 3.16). These could be formed by fecal waste of parrot fishes and/or urchins among others. The crustose red algae in 20-25 cm, trapped mud when it grew and it is possible to see the dark color of the sediments (Fig. 3.17). Mud sizes may have produced by mechanical breakdown of *Halimeda sp.* and *Cliona sp.* bored ships (Scoffin, 1987). Another way in which sediment is preserved is creating geopetals. Approximately 23 geopetals were identified in this core, mainly inside borings. All of them showed horizontal oriented deposition compared to the up orientation arrow.

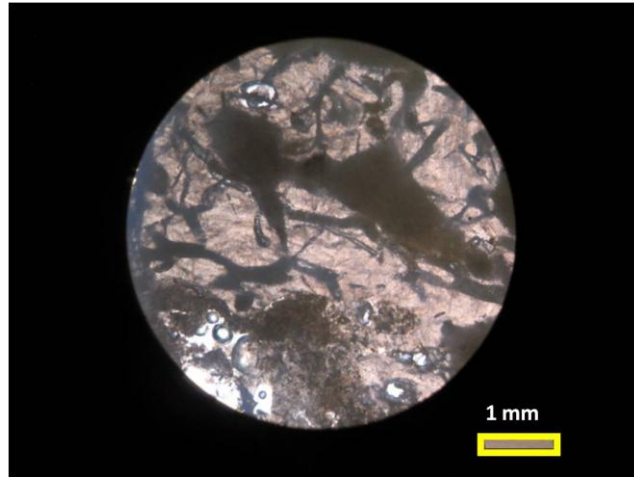


Figure 3.15. A piece of coral rubble with borings filled with mud (core interval: 0-20 cm).

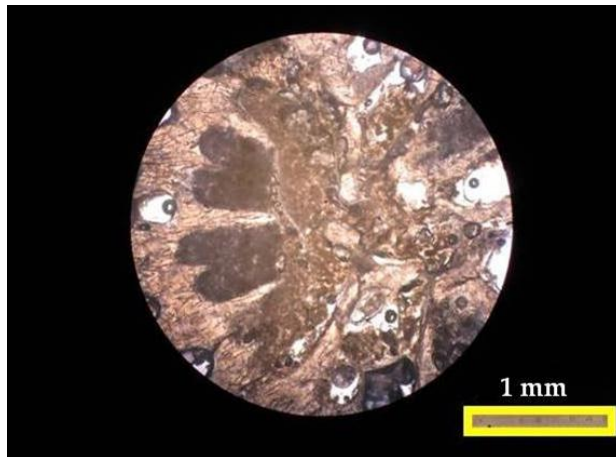


Figure 3.16. Mud and peloids in a *M. annularis* complex coral fragment (core depth: 120 cm).

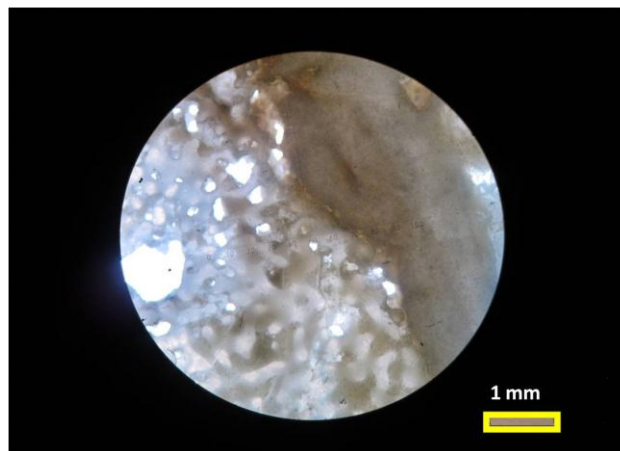


Figure 3.17. Crustose coralline algae located on top of an *A. palmata* fragment (top of the core).

In LP-2, sand-sized sediments were present inside a coral rubble fragment (acroporid), (Fig. 3.18), at around 25 cm; and also inside an *A. palmata* fragment internal structure (79-87 cm) (Fig. 3.19); where mud also was trapped. Crustose coralline algae also were found to have trapped fine sediments at around 40 cm. Sand sediments and possible fecal wastes were also documented in this core. A total of 4 geopetals were found, one of them in *A. palmata* fragment shows that, at least, after the boring was filled this piece of coral has not been transported (Fig. 3.20). Nevertheless, the coral fragment in interval 25-60 cm shows an inverted geopetal (Fig. 3.21) suggesting transportation and deposition.

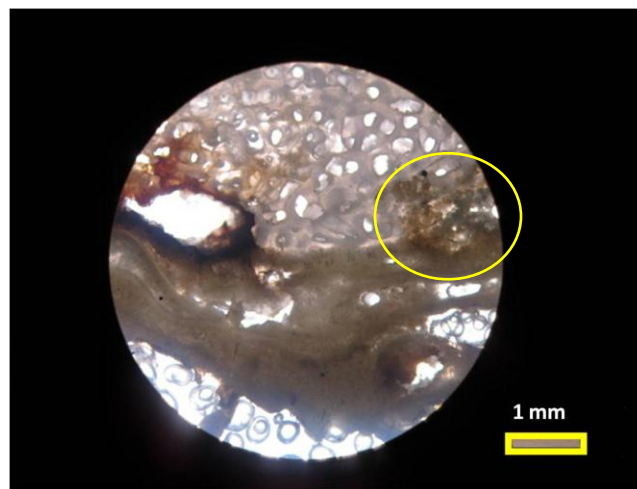


Figure 3.18. At the center right of the photo sand sized sediments (core depth: 25 cm).

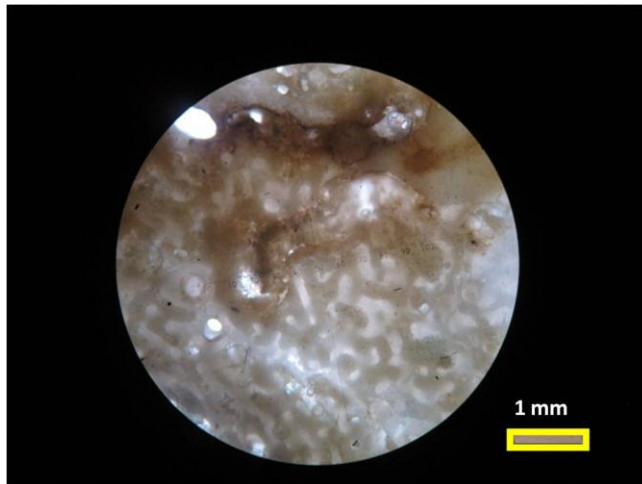


Figure 3.19. Sediments inside internal structure of an *A. palmata* coral fragment (core depth: 79-87 cm).

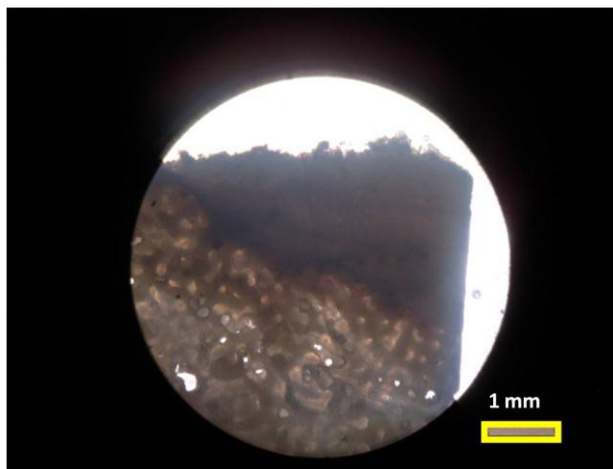


Figure 3.20. Horizontally oriented geopetal in *A. palmata* fragment at the core depth of 79 to 87 cm.

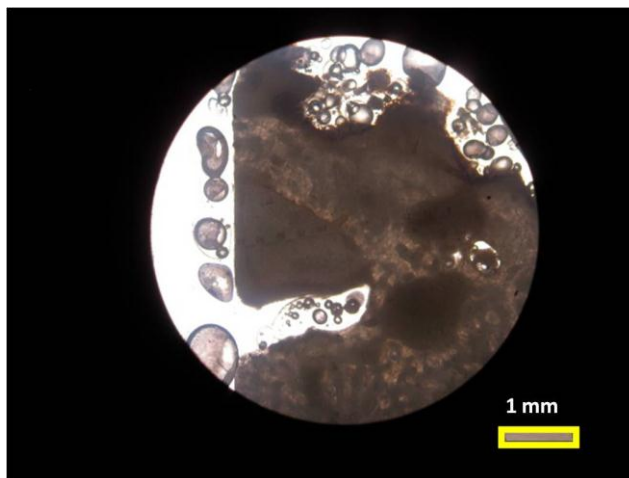


Figure 3.21. Inverted geopetal in *A. palmata* coral fragment at core interval: 25-60 cm.

In Core LP-3, sand was also documented inside a *M. annularis* complex internal structure at ~10 cm (Fig. 3.22). Sand was present inside the internal structure of the *Colpophillia* sp. coral fragment located at about 55 cm in the core. These sediments suggest a relatively higher energy location. Figure 3.23 shows a boring where many particles have been deposited, some identified as bryozoan skeletal fragments.

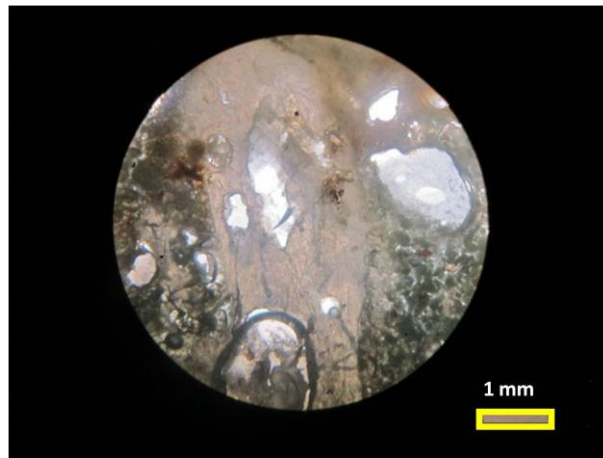


Figure 3.22. Sand-sized sediments located in a *M. annularis* complex fragment (core depth: 10 cm).

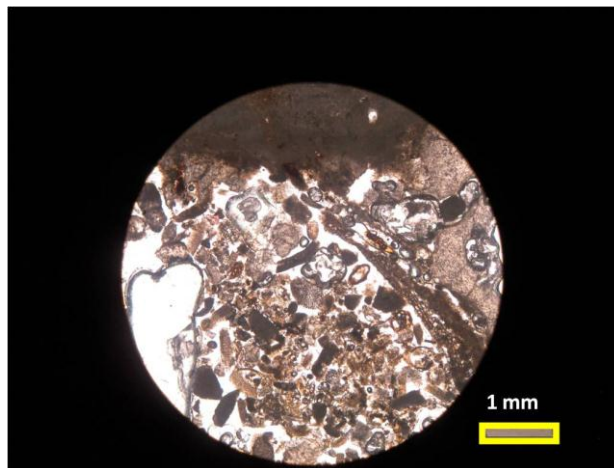


Figure 3.23. Clasts (mostly skeletal fragments) deposited in a boring at the top of the core (0-3 cm).

In LP-3A, sand sediments were also found inside the skeleton of a recent *A. palmata* fragment located at about 7 cm (Fig. 3.24). Another *M. annularis* complex coral skeleton fragment (~135 cm) had mud associated with borings as well as foram skeletons that were probably associated with the mud (Fig. 3.25). A total of 26 geopetals were identified in this core, most of them in the *M. annularis* complex coral fragments located in intervals from 36-114 cm. Figure 3.26 shows borings were geopetals have been formed.

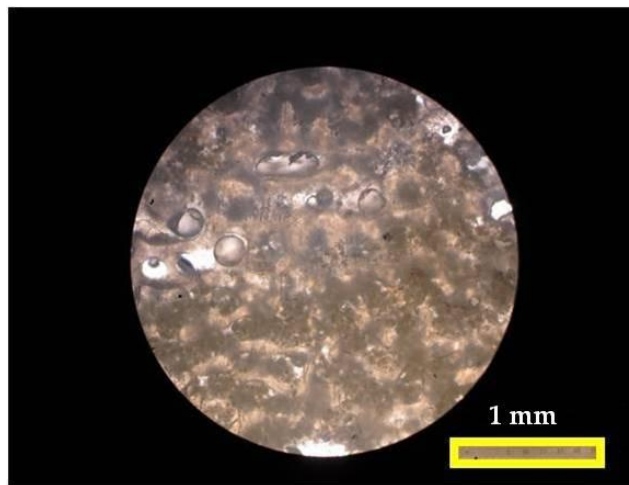


Figure 3.24. Sand in *A. palmata* internal structure at the top of the core.



Figure 3.25. Mud in boring includes some benthic forams (core depth: 135 cm).



Figure 3.26. Borings as geopetals (1 mm to 5 cm) at *M. annularis* complex fragment in LP-3A (core interval 70-114 cm).

3.1.3 Cores bioerosion descriptions

Bioerosion was probably one of the easiest events recorded in the core materials. Signs of this process were present everywhere in different shapes and sizes. All of these differences respond to different organisms, most of them boring clams (i.e. *Lithophaga sp.*), boring worms (serpulids) and boring sponges (i.e. *Cliona sp.*).

In core LP-1, borings diameters ranged from 0.5 mm to 4.0 cm and could get as deep as 5 cm inside the coral fragment. Relatively bigger diameters (1-4 cm) were common in bigger coral fragments, while smaller diameters (mostly 1 mm or less) were more common in coral rubble fragments. Figure 3.27 shows abundant borings (less than 1 mm) in a piece of coral rubble in

core LP-1 at the interval 20-25 cm. These borings are commonly produced by the boring sponges *Cliona sp.* which are one of the most important boring sponges in Caribbean reefs (Humann and DeLoach, 1994; Reis and Leão, 2000).

Microboring analysis, using point counting in thin sections (5X), showed some variability not only within samples of the same core, but also in the same thin section. Microboring term is used in this study to refer to borings seen in thin section, typically 3 mm or less. In different thin sections samples, microboring percentage varied from 23-24 to 80-82. The highest values were found in a sample of a *M. annularis* complex coral (80-82%) at the bottom of the core (148-149 cm) and also in a coral rubble piece (60-80%) located 10-15 cm from the top of the core (Fig 3.28).

Macroborings term is referred to borings that can be identified at naked eye, typically from 5 mm to few centimeters. Analysis of macroborings (hand samples) showed variability of 16% to 55 %, being the highest percentage of bioerosion identified in samples stratigraphically lowermost in the core (153 cm). Point counting to this sample showed 30 % more microborings (80-82 %) than macroborings (55 %). In interval 80-125 cm the *M. annularis* complex coral fragments showed 16-36 % of bioerosion and in the interval from 50-80 cm it was 32 %.



Figure 3.27. A piece of coral rubble at LP-1 with many (more than 40) small borings (1 mm and less) (core interval: 20-25 cm).

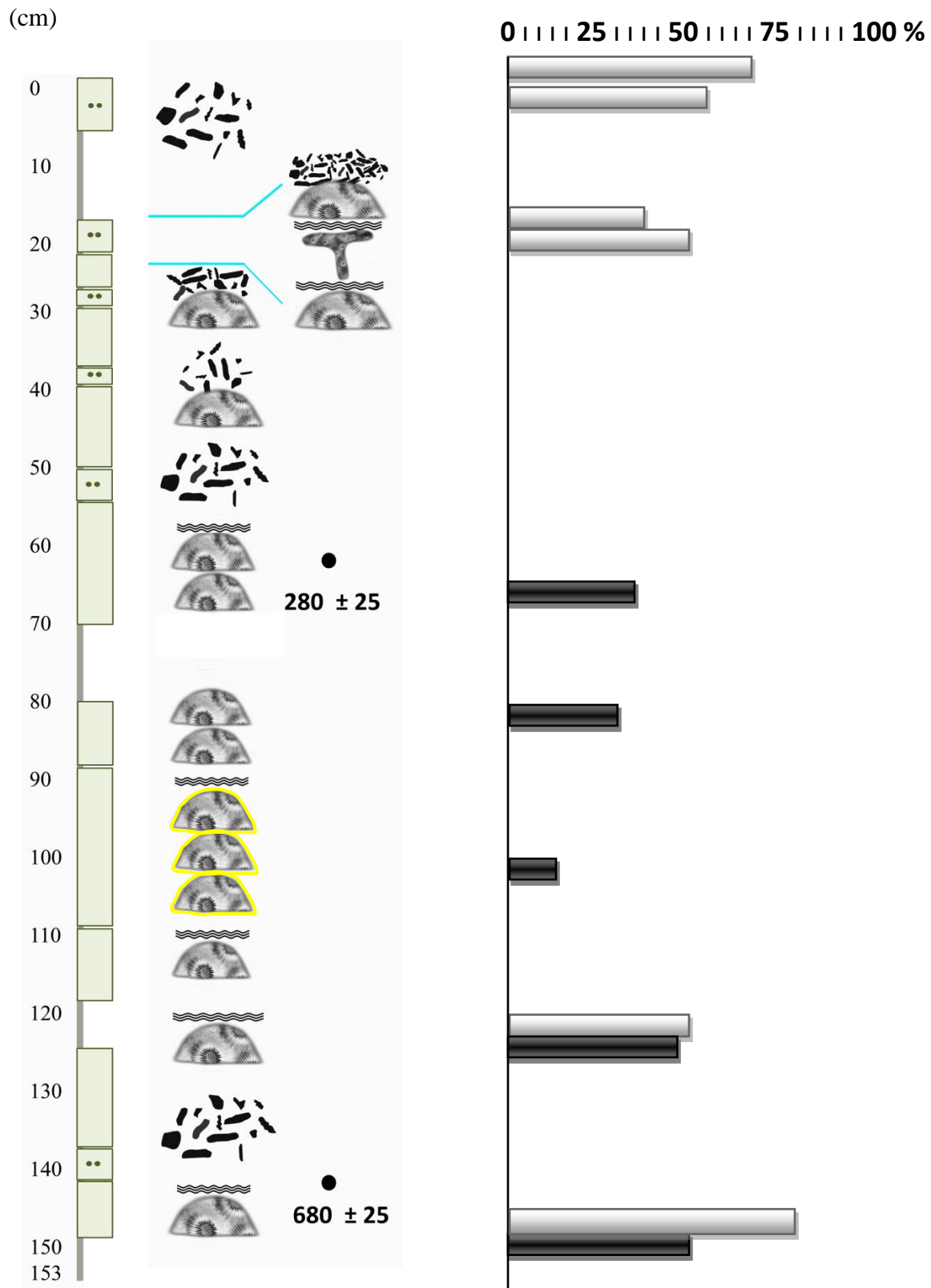


Figure 3.28. Macroboring (black bars) and microboring (gray bars) percentage in LP-1 content.

In core LP-2, bioerosion was also evident. Coral rubble fragments were visibly perforated (0.5 mm to 1.2 cm), probably by *Cliona sp.* sponges and other organisms. Some coral fragments show wider (up to 1.8 cm) borings created by *Lithophaga sp.* bivalves. Borings got as deep as 4 cm in this *A. palmata* coral fragment. In thin section analysis many other borings were identified ranging from 1 to 2 mm.

Analysis of microborings (less than 3 mm) based on point counts showed a range in the percentage covered by bores from 22 to 71 % in different samples of this core. The lowest values were identified in rubble pieces (22 %), but the higher values were found not only in rubble pieces at the top of the core (62-71 %) but in coral fragment (60-68 %) at the bottom (Fig. 3.29).

Macroborings percentage showed relatively lower values compare to microborings, ranging from 28 to 36 %. A *M. annularis* complex fragment at 79-87 cm, showed 20 % more microborings (50-70%) than macroborings (36%). Figure 3.30 shows an *A. palmata* coral fragment with 36 % of macroborings identified.

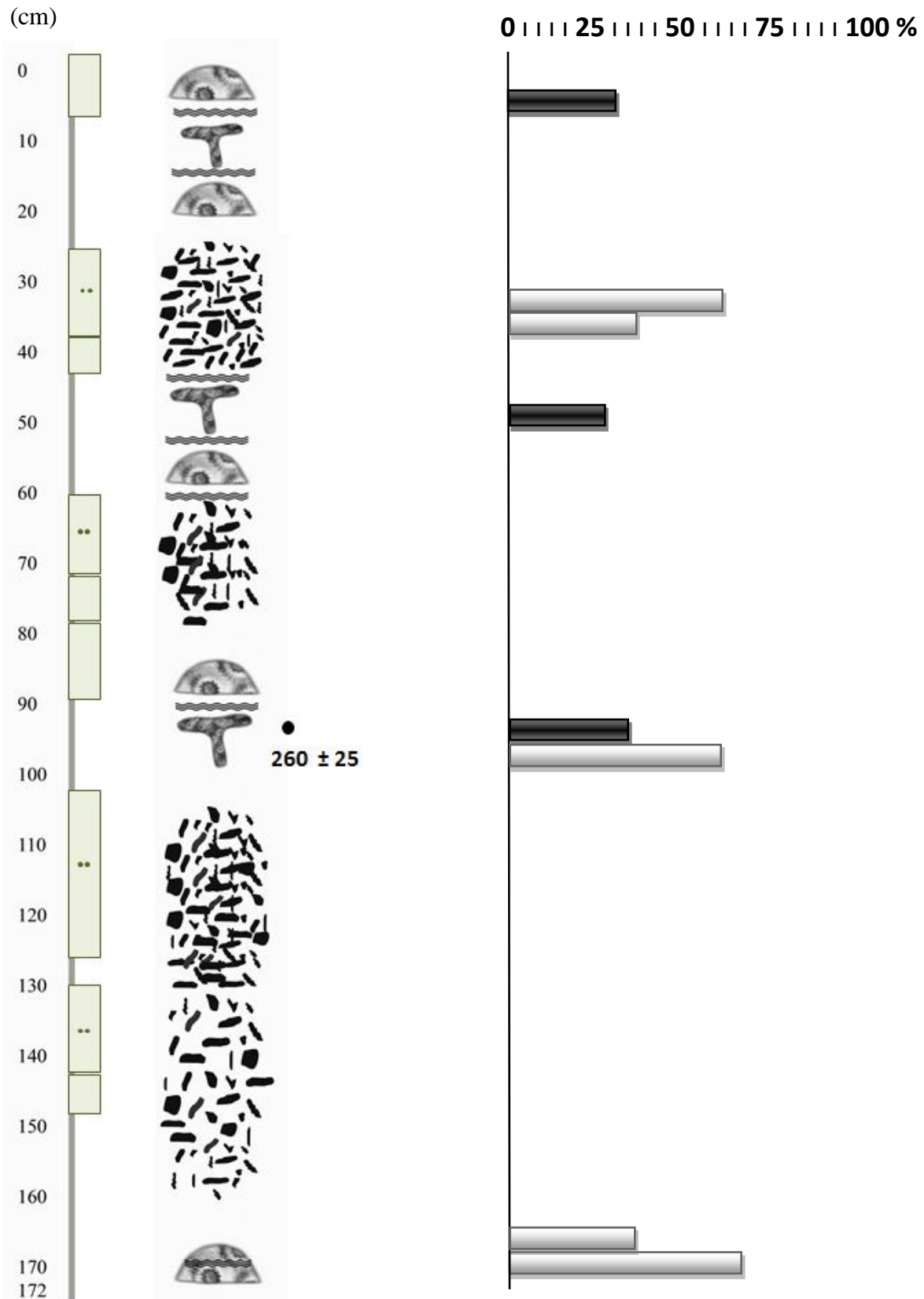


Figure 3.29. Macroboring (black bars) and microboring (gray bars) percentage in LP-2 content.



Figure 3.30. Borings (1 mm to 1.8 cm), some created by *Lithophaga sp.* in *A. palmata* coral fragment at 60-103 cm core interval.

In core LP-3 all the corals were perforated mostly by sponges. Figure 3.31 show the *M. annularis* complex coral fragment located at the top of the core with many small (1 – 2 mm) borings caused by *Cliona sp.*. In figure 3.32 pieces of coral rubble show many small borings. Overall, the range in diameter of the borings is from 0.5 mm to 1.5 cm, the latter found in a *M. annularis* complex coral fragment at the bottom of the core.

Microboring analyses showed values from 58 to 71 % in samples of rubble and coral fragments. This range of values is narrow and shows a high consistency in the percentage of boring along the core. The highest values were found at sample at the top of the core with 68-71 %. Macroboring was analyzed in one sample which resulted in 43.3 % bioeroded, about 30 % less than microborings (Fig. 3.33).



Figure 3.31. *M. annularis* complex coral fragment with abundant borings (stratigraphic top of the core located at the surface of the reef).



Figure 3.32. Coral rubble fragments with abundant borings (core interval: 0-28 cm).

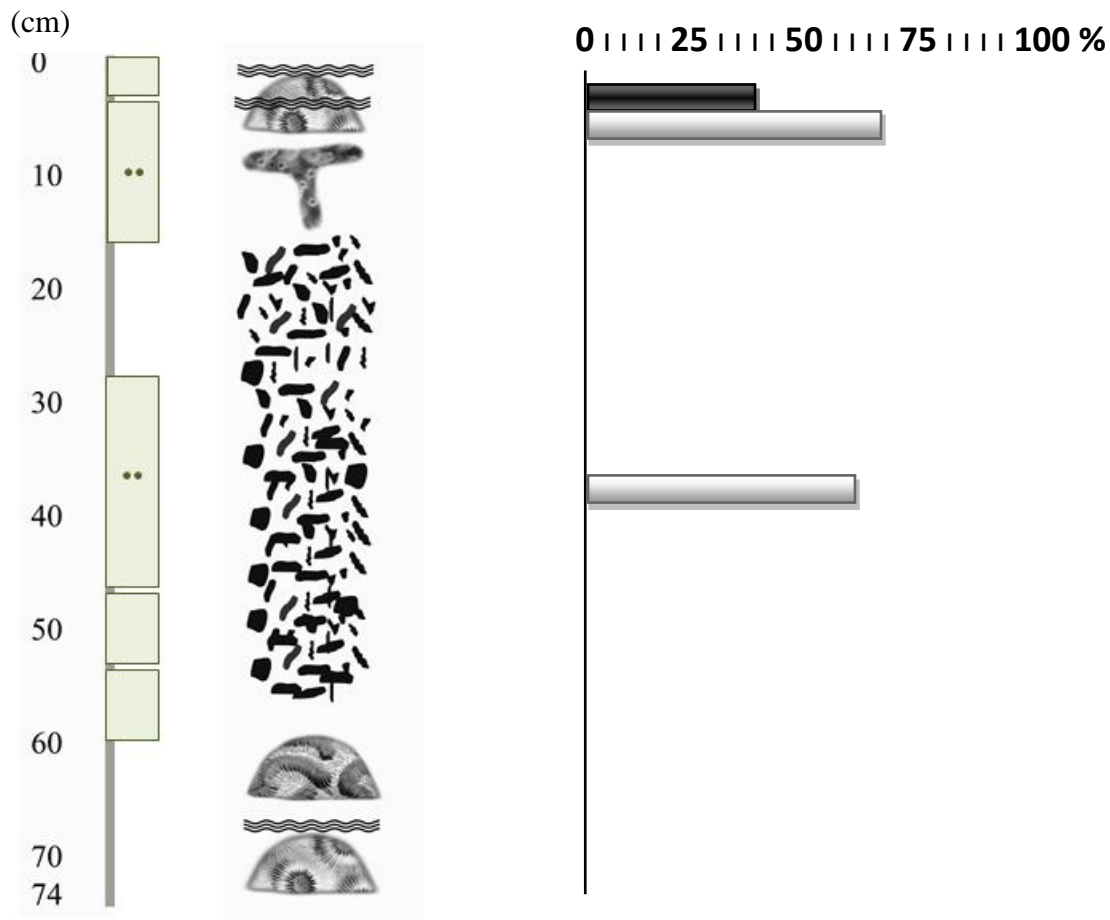


Figure 3.33. Macroboring (black bars) and microboring (gray bars) percentage in LP-3 content.

Larger borings (up to 5 cm) found in core LP-3A are attributable to *Lithophaga sp.* which was found in some coral fragments of this core. Figure 3.34 show borings produced by this bivalve in *M. annularis* complex at interval 36-70 cm. Diameters ranged 0.5 mm to 5 cm through all the core content.

Microborings percentages were relatively similar (37 to 52 %) throughout different samples, but in this core no relatively higher values (>60 %) were obtained. However, macroborings analysis showed relatively lower values in borings percentage from 26 % to 65 %, the latter obtained from a coral of *M. annularis* complex located at the bottom of the core. This is

a 20 % more compared with the microborings percentage (40 %) studied in this sample thin section (Fig. 3.35). A serpulid worm tube is shown in figure 3.37 identified in thin section analysis.



Figure 3.34. *Lithophaga sp.* located in boring (1 mm to 2.5 cm) while other borings are visible around (core LP-3A interval: 36-70 cm).

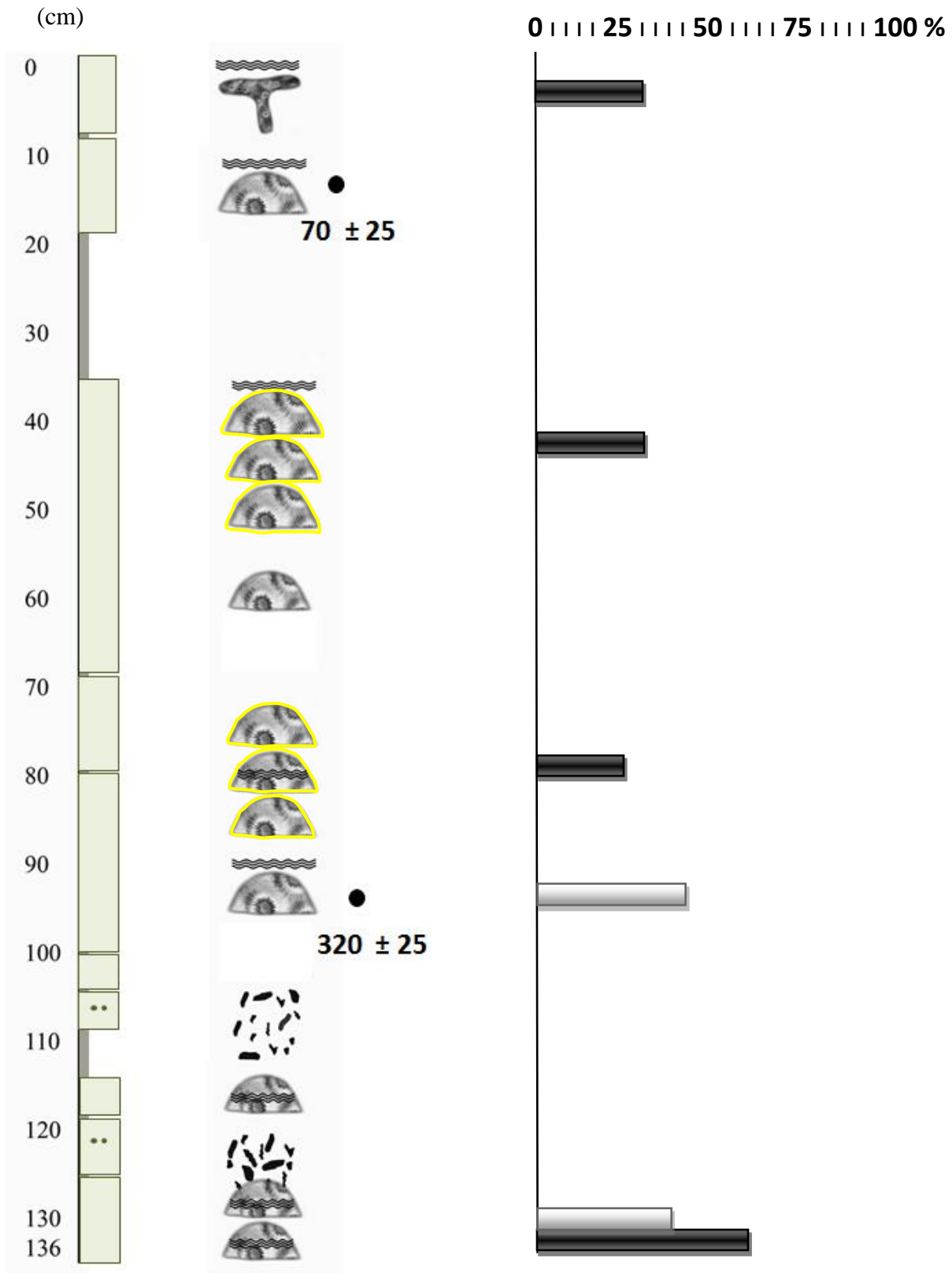


Figure 3.35. Macroboring (black bars) and microboring (gray bars) percentage in LP-3A content.

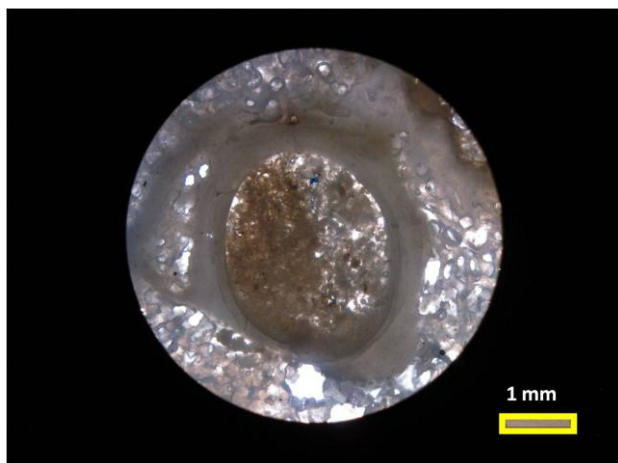


Figure 3.36. Serpulid tube located in *A. palmata* coral fragment at the top of the core.

3.2 Accretion rates

Accretion rates were calculated by subtracting calibrated radiocarbon ages and corals core depth (Table 3.1, Fig. 3.37). The accretion rates ranged from 1.1 to 3.4 m/ky resulting very close to the accretion rates cited in the literature for similar reef systems which is about 1.0-3.0 m/ky (Tucker and Wright, 1990). The high end of the calculated accretion rate in LP-3A and LP-2 (3.4 m/ky and 3.3 m/ky) was higher than the rest of the studied cores and higher than some examples in the literature. The recovery in LP-3A core is composed mostly of a single colony of *M. annularis* complex. However, in core LP-2, the accretion rate is the result of coral fragments and coral rubble accumulation. In core LP-1 the lowest accretion rate was obtained probably because coral growth rate was less compared with coral growth in LP-3A. This represents an accretion rate of 1.1 m/ky and it is the lowest for all cores. Many interrelated factors are involved in the accretion rate of a reef system and different areas are expected to accrete at different rates. Variations in accretion rates are expected due to differences in the dynamics of construction and destruction processes as well as preservation. In Hubbard et al. (1997) the core material

recovered at the shelf edge reefs indicated a stop in reef accretion format about 5,000 to 6,000 yrs. This study documents recent accretion in the outer shelf in the last 700 years.

Table 3.1. Accretion rates calculated from radiocarbon ages from corals located at different intervals along the cores.

Description	Core	Interval (cm)	14 C age yr BP	Accretion rate (m/ky)
<i>M. annularis</i> complex	LP-1	69-0	280 ± 25	2.4
<i>M. annularis</i> complex	LP-1	146-69	680 ± 25	1.1
<i>A. palmata</i>	LP-2	87-0	260 ± 25	3.3
<i>M. annularis</i> complex	LP-3A	10-0	70 ± 25	1.4
<i>M. annularis</i> complex	LP-3A	110-10	320 ± 25	3.4

Figure 3.38 shows a stratigraphic correlation in three of the four cores (LP-1, LP-2 and LP-3A). The basis of this correlation is the radiocarbon ages obtained from corals, ranging from 280 to 320 ± 25 yrs which indicate a similar geologic time. It is evidenced that accretion was occurring at that time in these three cores. As time lapsed different content was deposited in each case; a coral fragment in LP-1, coral rubble in LP-2 and colonization (coral growth) in LP-3A. This demonstrates the high variability in these reefs which are relatively close one to another (less than 1 km apart).

If it is assumed that accretion rates vary through the reef depth (2-4 m) at a similar rate measured in this study, then the spurs could have started to form around 1,000 to 2,000 years ago. Knowing that accretion rates are variable, this only represents an average time of formation of these spurs. Other spurs in the vicinity may have formed early or later.

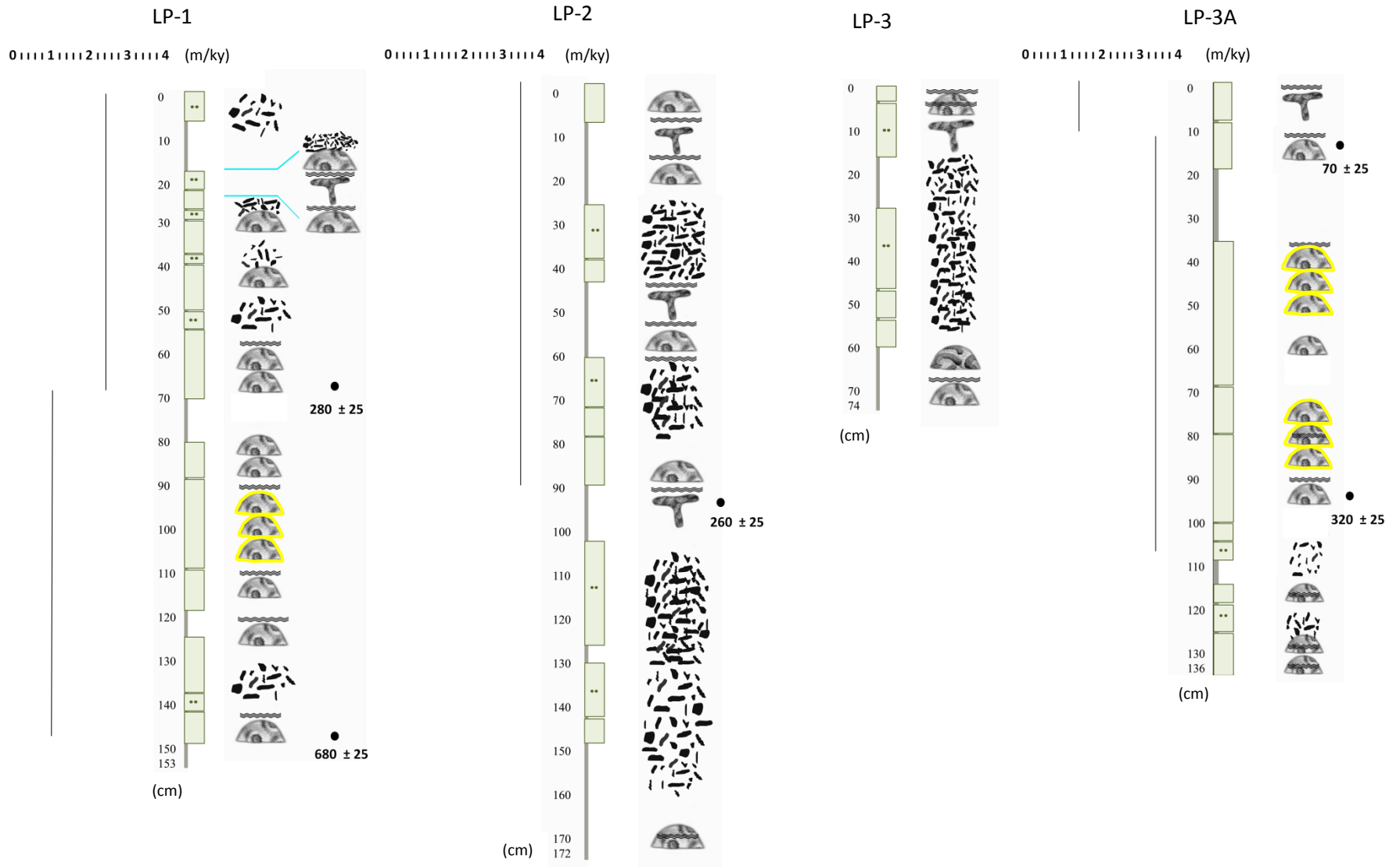


Figure 3.37. Stratigraphic columns of the cores showing the accretion rates.

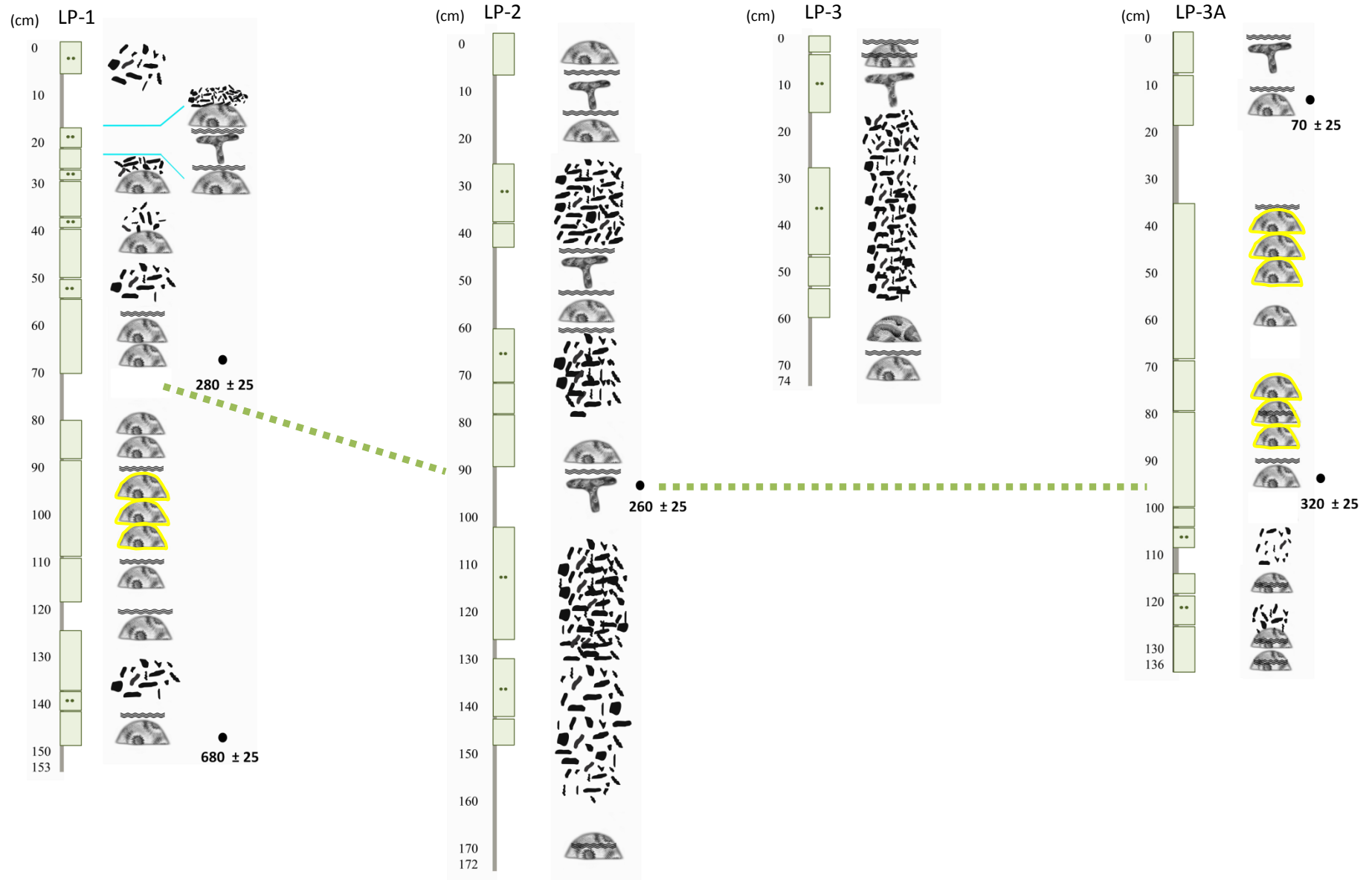


Figure 3.38. Stratigraphic correlation using radiocarbon ages (260 to 320 ± 25 ybp) in three cores.

3.3 Accretion rates in the Caribbean

Accretion rates have been documented in several reefs in the Caribbean including Jamaica, Florida, St. Croix, Puerto Rico and México. Table 3.2 shows different reef locations and their correspondent accretion rates. There is variability between each Caribbean reef location and some of these accretion rates are biases since they represent recovery of continuous coral colonies in growth position such as in *A. palmata* and *M. annularis* complex. Hubbard et al., (1997) accretion rates in cores collected from different parts of the platform in southwest Puerto Rico (inner shelf, mid shelf and shelf edge in Parguera) also show high variability. However, when comparing the accretion rates in this study (1.1 to 3.4 m/ky), with the other studies cited in the results have a high degree of similarity. During the last 2,000 years sea level has risen about a meter per thousand years (Fig. 1.2) and core data showed a mean accretion rate of 2.3 m/ky. In general, these reefs were accreting similarly to sea level rate.

Table 3.2. Reef accretion rates in different Caribbean reefs.

Reef location	Reef description	Depth range (m)	Accretion rate (m/ky)	Reference
México	Spur and groove	0-2	0.2 – 2.0	Blanchon and Perry, 2004
Florida	Spur and groove	2-9	0.6 - 1.0	Shinn et al, 1977
Jamaica	Fore reef	17	0.55 - 1.0	Land, 1974
St. Croix	Shelf edge (Lang Bank)	12.2 – 16.6	2.8 – 13.5	Hubbard et al., 1997
Puerto Rico	Shelf edge (Parguera)	7.4 – 10.4	2.3 – 9.6	Hubbard et al., 1997
Puerto Rico	Mid shelf (Parguera)	10.3 – 12.5	0.1 – 4.2	Hubbard et al., 1997
Puerto Rico	Inner shelf (Parguera)	1.4 – 5.9	2.7 – 14.7	Hubbard et al., 1997
Puerto Rico	Spur and groove	14	1.1 – 3.4	This study

3.4 Interpretation

With the exception of LP-1, all the cores contain *A. palmata* at the top, but these pieces are clasts that could have experienced some transport, same for some *M. annularis* complex coral fragments. Continuous recovery of *A. palmata* but this was not found. All coral fragments recovered account for a 27% (LP-3) up to 73% (LP-3A) content in the cores, a high variability within the same spur reef, since specifically these two cores belong to the same reef setting.

Two of the four cores studied (LP-1 and LP-3A) contain *M. annularis* complex coral skeletons massive enough and with the corallites orientations suggesting growth position, a fact that suggests they are part of the reef framework. The two intervals where this is located are at ~50 to ~125 cm in LP-1 and at ~36 to ~114 cm in LP-3A; representing a 20 % and a 50% of the core recovery respectively. In these intervals continuous colonies of *M. annularis* complex (probably *Montastrea faveolata*) show a significantly different texture and composition compared to most of the material recovered from the rest of the cores which are chaotic, composed of fragments and probably representing secondary framework. Also, by observing these samples it is possible to see part of other colonies that may resemble the columnar shape of the species or adjacent colonies. Although, growth position colonies were identified using the characteristics previously mentioned, some other *M. annularis* complex coral fragments recovered in the cores could have been in growth position, for example in LP-1 at 70 cm and also at 80 cm. In these samples the coral fragments are well preserved and corallites orientations suggest growth position, but these are relatively smaller samples (10- 15 cm length). As this one, there were also some other fragments where the coring procedure seem to have altered the recovery by cutting adjacent coral colonies along their irregular edges and making them look out

of place. These observations suggest that the "in situ" percentages provided in this study could be underestimated due to the sampling procedure.

Overall there is variable amount of coral rubble (7% in LP-3A to 68% in LP-3), mostly branching type, and other broken pieces of massive type. The rubble content represents the sum of mechanical breakdown, caused by wave and storms action, and bioerosion processes, which is acting at all times in the reef. These rubble sediments commonly accumulate in crevices, flat areas and other reef structure irregularities (Fig. 3.39). Most of the identifiable coral rubble was composed of fragments of *A. cervicornis*, a branching delicate coral vulnerable to break down during storms and hurricanes (Rasser and Riegl, 2002), which can be found today at some spurs alive. The fact that most of the *A. cervicornis* rubble is being documented for up to 600 hundreds of years in this study suggests the presence of this coral in these spurs through this time.

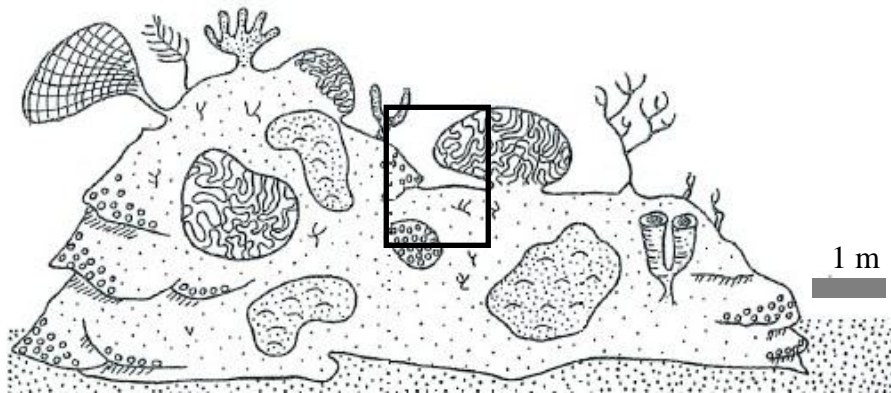


Figure 3.39. Reef diagram showing possible area were rubble can accumulate. Modified from Scoffin, 1987.

A minor component present was crustose coralline algae (1% in LP-1 to 5% in LP-3A). Although most of these algae layers were located on top of the corals there were cases in which they were located within the coral, interpreted as interruptions in the coral growth maybe because environment was not suitable for coral growth but positive for algae growth. Another

observation about the crustose algae zones is the thickness increase during the last 300 yrs approximately in two cores (LP-2 and LP-3A). Some factors known to promote red algae growth include: irradiance, temperature and sometimes nitrogen limited (Wai and Williams, 2005). The differences in thickness may indicate timing differences in coral recolonization and/or differences in the environment that promoted or negatively affected algal growth. In summary, the cores content recovered from these reefs are mostly composed of coral fragments (48%), followed by coral rubble (33%), in situ corals (17%) and crustose coralline algae (2%). This results in similar findings with other studies (Hubbard et al., 1998) whose found framework be uncommon in cores recoveries in some Caribbean reefs.

In terms of bioerosion there were relatively higher values (62-80%) of microborings at the top of three of the cores (LP-1, LP-2, LP-3). Similar relatively higher values (60-82 %) were identified in samples at the bottom of two of these cores (LP-1 and LP-2) suggesting that similar conditions occurred before. Serpulid worms tubes diameters (2 mm and less) and its abundances in each core (from 53 to more than 100 tubes in the different cores, more abundant in rubble substrates) are exerting an important control in bioeroding the corals and probably accounting for the higher percentages of microborings in the studied samples but also aided by other organisms like sponges. Serpulid worms could be related to nutrient availability (Hutchings and Peyrot-Clausade, 2001), since these organisms are filter fed. The range in the percentage covered by bores may indicate conditions suitable for bioeroders to abound or submarine exposure of the material for a "longer" time.

Macroborings were in general relatively lower, up to 30 %, compared with microborings. Only one sample at the bottom of LP-3A core, showed 20 % more macroborings than its thin

section sample. Most of which have been caused by *Lithophaga sp.* This recognizes the microboring organisms' importance in bioerosion.

The cements found are typical of subtidal environments. Micritic cement found in *A. palmata* (LP-2) fragments could indicate metabolic and processes associated to bacteria and algae, breakdown or micritization of calcareous algae skeletons forming fine grained deposits, boring activities of some organisms and or authigenic precipitation. Bioerosion caused by marine organisms and grazers is also an important process in producing clay and silt carbonate grains which can contribute to micrite formation (Flügel, 2004). Interparticle cementation was more evident in core LP-2 where it account for 20% of the coral fragments recovered. In general, cementation in coral rubble pieces was minimum, limited to few pieces and aided by algae encrustations, which were dominant in all cores rubble zones. Less interparticle cementation were evidenced in LP-3A, however intraparticle was found in corallites.

4.0 CONCLUSIONS

Three major constituents were found in four cores from the outer shelf in southwest Puerto Rico: *M. annularis complex* coral fragments, *Acropora palmata* coral fragments, and coral rubble. This study documents the *M. annularis complex* coral as a main reef builder during the last 700 years while recoveries of *A. palmata* specimens were mostly in the form of fragments and not in place. Also, the content of these cores show detritus produced in the spur and groove reef like *A. palmata* coral fragments and *A. cervicornis* rubble, which are broken and deposited during strong current or storms in the outer shelf. Dead *A. palmata* colonies (in growth position) have been found at some spurs with little or no living tissue and could represent the source of these coral fragments in the cores. Total recovery show most of the content composed of coral fragments (48%), followed by coral rubble (33%), in situ corals (17%) and crustose coralline algae (2%). Bioerosion was mainly controlled by organisms such as *Lithophaga sp.*, sponges and serpulid worms, being the last two more important in removing coral material. Cementation processes vary within spurs and is more evident in coral fragments than in coral rubble. Radiocarbon ages indicate ages of the corals from 70 to 680 ± 25 ybp. Therefore, recent accretion rate is documented for the first time in the outer shelf, were other studies reported little or no accretion during the last 6,000 years. The average accretion rate obtained in this study (2.3 m/ky) represent average values in the literature and are also similar with other Caribbean reef accretion rates. The formation of the spur studied could have been started at least 1,000 to 2,000 years ago.

5.0 FUTURE WORK

Currently Edgardo J. Quiñones Cruz, a geology graduate student at UPRM, is studying samples of *M. annularis* complex corals of these cores to obtain paleo-temperatures records. Also, more cores are being recovered from adjacent spurs. The incorporation of these data to this study will serve to understand changes in the environment during the last thousand years. Coral growth rates also in relation to time and to the environmental parameters should also be studied. In addition, detailed bioerosion data should be worked in terms of total carbonate loss and the species involved in the removal. In this way a carbonate budget for the area could be developed.

APPENDIX A: Cores Detailed Descriptions

Core LP-1

Core Interval

0-20 cm

This interval is mostly composed of coral rubble. There are 17 pieces of mostly highly encrusted *A. cervicornis* (sizes varied between 2.5 to 8 cm long). In general, these fragments are angular to subangular. Crustose red algae was present along with encrusted foram *Homotrema rubrum*, three serpulid tubes (<1 mm to 1 mm diameter), urchin spines and borings (0.5 – 3 mm) all over. Fragments of sponges were also found. Sparite cement and mud found by thin section analysis in one of the fragments.

20-25 cm

This interval is composed of coral rubble on top and a coral fragment which contains, *M. annularis* complex, an *A. palmata* below and last, another *M. annularis* complex. There are 73 pieces, shorter and subrounded compared to the rubble of the first interval (sizes varied between 1 to 5 cm long). Some of these fragments are *A. cervicornis* while there are many other pieces that are not possible to identify only by hand-sample. Encrusted foram *H. rubrum*, serpulid tubes (<1mm to 1mm diameter) and borings (<1 mm to 0.5 cm) were also found in the rubble. A cup coral was found attached to an *A. cervicornis* piece.

In the coral fragment (5 cm long), the two species found were possible to identify by thin section analysis (*M. annularis* complex on top, followed by *A. palmata*, and *M. annularis* complex below). Two crustose red algae layers (thickness: 2 mm and 3 mm) were found in this fragment separating the coral species. Mud was trapped by this algae. In the *M. annularis* complex at the top peloids were found in borings and fragments of *Halimeda sp.* were found in other cavities. Encrusted foram *H. rubrum*, 1 serpulid tube (1mm diameter), urchin spines, and borings (1 mm to 1.3 cm) are also present. A fragment of *A. cervicornis* is cemented to this coral fragment. No geopetals were found.

25-33 cm

This interval is composed of coral rubble and a coral fragment below. There are 15 pieces of mostly *A. cervicornis* (sizes varied between 1-4 cm long). Encrusted foram *H. rubrum*, serpulid tubes (< 1 mm diameter) and borings (<1 mm to 1 mm) are present. These pieces are rounded to subrounded.

In the coral fragment (8 cm long), a *Lithophaga* sp. was found inside a burrow. Encrusted foram *H. rubrum*, 5 serpulid tubes (<1 mm to 1 mm diameter) and borings (1 mm to 1.5 cm) are present. Filled cavities were found, but any geopetals.

33-50 cm

This interval is composed of coral rubble and a coral fragment below. There are seven pieces of mostly encrusted *A. cervicornis* (sizes varied between 1.5-6 cm long). These fragments are mostly subangular. Serpulid tubes (< 1 mm diameter) and borings (1 mm to 1 mm) are present.

In the coral fragment (10 cm long), encrusted *H. rubrum*, small gastropods, small *Lithophaga* sp., three geopetals were found and micrite (brown areas). Four serpulid tubes (<1 mm to 1 mm diameter) and borings (1 mm to 3 cm) were found.

50-80 cm

This interval is composed of coral rubble and two pieces of *M. annularis* complex. There are 32 pieces of mainly encrusted *A. cervicornis* (sizes varied between 1-4 cm long), other species difficult to identify are also present. These pieces are subangular to subrounded. Encrusted *H. rubrum*, gastropods, serpulid tubes (< 1 mm to 1 mm diameter), borings (<1 mm to 2 mm) urchin spines are also present.

A *M. annularis* complex coral fragment (7 cm long), is located below and contains encrusted *H. rubrum*, 8 serpulid tubes (< 1 mm to 2mm), urchin spines and borings (1mm to 1 cm).

A *M. annularis* complex coral fragment (16 cm) is located at the bottom of this interval. It contains encrusted *H. rubrum*, a layer of crustose red algae on top (thickness: 4 mm), filled cavities and micrite. Ten geopetals were found in this fragment, all of them horizontally oriented. Four serpulid tubes (<1 mm to 2 mm) and borings (1 mm to 1 cm, and up to 3 cm long). Radiocarbon age in this sample resulted in 665 ± 25 yrs.

80-125 cm

This interval is composed mainly of massive coral *M. annularis* complex. Three coral fragments make this interval. The first *M. annularis* complex (8.5 cm long) contains *Halimeda* sp., *H. rubrum*, *Lithophaga* sp., six serpulid tubes (< 1 mm to 2 mm), urchin spines, borings (1 mm to 4 cm), micrite, fine sediments and black spots, four geopetals horizontally oriented. A single piece of *A. cervicornis* is found in this interval.

The second coral fragment of *M. annularis* complex (20.5 cm long) contained relatively few *H. rubrum*, 7 serpulid tubes (< 1mm to 1 mm), borings (1 mm to 2.5 cm), five geopetals horizontally oriented, urchin spines, a layer of crustose red algae on top (thickness: 2mm), micrite and black spots.

A third coral fragment of *M. annularis* complex (9.5 cm long), at the bottom of this interval, contains articulate red algae, a layer of crustose red algae on top (thickness: 3 mm), 5 serpulid tubes (< 1mm to 1 mm), borings (1 mm to 1.3 cm), micrite and black spots. Micritic, acicular, sparite and botroidal cements were found by thin section analysis, as well as peloids, other sediments and forams.

125-153 cm

This interval was composed of a *M. annularis* complex coral fragment (12.5 cm long) on top, coral rubble below and another *M. annularis* complex coral fragment at the bottom of the core. The first *M. annularis* complex contains articulate red algae, crustose red algae on top (thickness: 1 mm), *H. rubrum*, 10 serpulid tubes (< 1 mm to 2 mm diameter), urchin spines, and also gastropod shells (including a Flamingo Tongue shell) were found in borings. Other components found: borings (1 mm to 2 cm) and gray colored coral sections and calcareous sediments. This coral fragment contains a coral fragment of *Diploria sp.* attached below.

The coral rubble is a group of 32 pieces; about eight identified as *A. cervicornis*, one as *M. annularis* complex and the rest of unknown origin, mostly encrusted. These fragments are subangular to rounded, vary in sizes (0.5cm-5cm long), few are preserved and contain many borings (1 mm to 2 mm).

The last coral fragment is a *M. annularis* complex (9 cm long), which contains organisms such as *H. rubrum* and fragments of others like 3 serpulid tubes (< 1mm to 1 mm diameter). Other components include: borings (1 mm to 2.5 cm) and also show a gray color. Acicular and bladed cement were found by thin section analysis. A crustose red algae layer is located at the top of this fragment with a thickness of 1 mm. Five geopetals were found horizontally oriented. Radiocarbon age in this sample resulted in $1,160 \pm 25$ yrs.

Core LP-2

Core Interval:

0-25 cm

In this interval, a *M. annularis* complex coral fragment is located on top of an *A. palmata* fragment followed by a *M. annularis* complex fragment. The species are divided by crustose red algae layers. The species are cemented making only one fragment (7 cm long). This was possible to identify by thin section analysis. There is presence of *Halimeda* sp., *H. rubrum*, 3 serpulid tubes (< 1 mm to 1 mm), urchin spines and borings (< 1 mm to 0.9 cm). This piece is micritized, shows black spot in the coral structure and some sediment is also present in voids. Two crustose red algae layer were identified in this fragment (thickness from bottom to top: 1 cm, 3 mm).

25-60 cm

This interval is composed of two parts, first a coral rubble zone of about 100 pieces, below it, a fragment of *A. palmata* cemented to a *M. annularis* complex fragment. In the coral rubble, approximately 40 out of those 100 pieces were identified as *A. cervicornis* fragments. In these pieces there was presence of *H. rubrum*, some gastropods, 6 serpulid tubes (1 mm diameter) and urchin spines. Also, borings (< 1 mm to 0.3 cm), some pieces dark colored and, in general, pieces were subrounded to subangular and encrusted. Possible micritic cement and sand found in one of the fragments by using thin section analysis as well as sand in borings.

The fragment (6 cm long) containing the *A. palmata* and *M. annularis* complex (below), has a crustose red algae layer on top (thickness: 1 mm), containing mud, another layer dividing the coral species (thickness: 1.5 cm) and another at the bottom (thickness: 2 mm). Sediments are present in the algae layers. Cemented to this coral fragment is a piece of *A. cervicornis* at the bottom. Also, borings (< 1 mm to 1.3 cm) were found. The identification of these two corals was possible by thin section analysis. An inverted geopetal was found in thin section analysis.

60-103 cm

In this interval, three parts were identified; first, a coral rubble zone of 40 pieces; second, and a *M. annularis* complex coral fragment and an *A. palmata* coral fragment below. In the coral rubble, 15 out of those 40 pieces were identified to belong to the *Acropora* genus also, a *Colpophillia* sp. piece and few cemented pieces of *A. cervicornis*. In these fragments, there is a presence of *H. rubrum*, more than 30 serpulid tubes (0.2 mm to 1 mm diameter), borings (<1 mm to 1.2 cm) and mostly, these pieces are subangular.

The *M. annularis* complex coral fragment (7.5 cm long) found below contains an *A. cervicornis* piece cemented to it. It also has presence of *H. rubrum*, 2 serpulid tubes (0.2 mm to 0.5 mm diameter), borings (< 1 mm to 0.5 cm), micritization and black spots in the coral structure.

The *A. palmata* fragment (11 cm long) contains three horizontally oriented geopetals, a layer of crustose red algae on top (thickness: 7 mm), more than 10 serpulid tubes (0.2 mm to 1 mm diameter) and borings (1 mm to 1.8 cm). Acicular and bladed cement found by using thin section analysis and also mud and sand sediments in borings. Radiocarbon age in this sample resulted in 630 ± 25 yrs.

103-130 cm

This interval is composed exclusively of coral rubble. There are two zones though; first approximately 140 pieces (14 acroporid pieces) of coral rubble and at the bottom some 5 cemented pieces of *A. cervicornis*. The group of fragments has many small borings (< 1 mm to 0.7 cm), about 28 serpulid tubes (0.1 to 1 mm diameter) is micritized and mostly these pieces are subrounded and rounded. The cemented pieces were identified as *A. cervicornis*. It contained articulate red algae, *H. rubrum*, 10 serpulid tubes (0.5 mm to 1 mm), borings (< 1 mm to 0.3 cm) and are gray colored. These fragments are subangular to rounded.

130-172 cm

This interval is composed of two parts: coral rubble and a *M. annularis* complex coral fragment below. There are 50 pieces of rubble, some of unknown id (some gray colored, some brown), a piece of *Colpophillia sp.*, eight pieces of *A. cervicornis* (some preserved, different sizes) and a bivalve shell. These fragments show borings (< 1 mm to 0.7 cm), 24 serpulid tubes (0.3 mm to 1 mm diameter), *H. rubrum* presence and are subangular to rounded.

Below is the *M. annularis* complex coral fragment (5 cm long), which has borings (<1 mm to 0.5 cm), 20 serpulid tubes (0.1 mm to 2 mm diameter), is gray colored, only has few corallites and contains a layer of crustose red algae at the middle of the fragment (thickness: 2 mm). Four geopetals were found horizontally oriented.

Core LP-3

Core Interval:

0-28 cm

This interval is composed of a *M. annularis* complex coral fragment on top, an *A. palmata* coral fragment below, followed by a zone of 31 pieces of coral rubble. The *M. annularis* complex fragment (2.5 cm long) contains mud and sand sediments, *H. rubrum*, 4 serpulid tubes (0.1 mm to 1 mm diameter), many borings (1 mm), the largest being about 1 cm. Also, there sponge fragments on top and a layer of crustose red algae (thickness: 6 mm). Another algae layer is found at the middle of the *M. annularis* complex coral (thickness: 2 mm).

The *A. palmata* fragment (3 cm long) contains borings (< 1 mm to 1 cm) and 3 serpulid tubes (0.2 mm to 1.5 mm). *H. rubrum* is present and the coral is micritized.

In the coral rubble, about eight pieces were identified as *A. cervicornis*, while much of it is unrecognizable. In these fragments there is presence of *H. rubrum*, 12 serpulid tubes (0.1 mm to 0.5 mm diameter), borings (1 mm), few fragments are cemented together, with different sizes (few preserved) and mostly are subangular to subrounded.

28-74 cm

This interval has three constituents: coral rubble on top, followed by a *Colpophillia sp.* fragment and a *M. annularis* complex fragment at the bottom of the core. The coral rubble zone has approximately 100 pieces, mostly *A. cervicornis*, others unrecognizable. Fragments are encrusted by red algae; also presence of *H. rubrum*, more than 40 serpulid tubes (1 mm-2 mm diameter), many small borings (1 mm) and few preserved pieces. The *A. cervicornis* fragments are 1cm to 1.5 cm thick and some of these pieces are cemented with others. In general, these fragments are subangular to angular, and few subrounded. Mud was found in a piece by thin section analysis.

The *Colpophillia sp.* fragment is 7 cm long, has many small borings (1mm), 4 serpulid tubes (1 mm to 2 mm diameter) and some sand sediment trapped in coral internal structure (thin section analysis).

At the bottom, the *M. annularis* complex fragment (5.5 cm long) was identified by thin section analysis since is not well preserved. It has a crustose red algae layer on top (thickness: 5 mm); also *H. rubrum* is present and contains borings (1 mm to 1.5 cm).

Core LP-3A

Core Interval:

0-36 cm

In this interval there are two parts: an *A. palmata* fragment at the top and a *M. annularis* complex fragment below. The *A. palmata* contains a layer of crustose red algae in its top (thickness: 2 cm), which contains sand and mud (thin section), also borings (< 1mm to 1.5 cm), 12 serpulid tubes (0.1 mm to 1 mm diameter), presence of sediments and shows black spots.

The *M. annularis* complex fragment shows 13 serpulid tubes (0.1 mm to 1 mm diameter), borings (< 1 mm to 1.5 cm), crustose red algae on top (thickness: 1 mm), and also black spots. Sediments and sponges are also present in this sample. Radiocarbon age in this sample resulted in 490 ± 25 yrs.

36-70 cm

This interval is composed exclusively of two *M. annularis* complex fragments. The first fragment is the biggest *M. annularis* complex found in all four cores, with 32 cm long. Some of the organisms found were: articulate red algae in borings, *Lithophaga sp.* and 18 serpulid tubes (0.1 mm to 1 mm diameter). Other features found include: 12 geopetals horizontally oriented, borings (1mm to 2.5 cm), some filled with sediments and also has black and orange colored spots. A layer of crustose red algae on top has a thickness of 2 mm.

At the bottom of this interval is another fragment (10.5 cm long) of *M. annularis* complex divided in two fragments. One of these fragments is about 10 cm long and contains an *A. cervicornis* piece (7.5 cm long) cemented to it. It also has 4 geopetals horizontally oriented and borings (< 0.5 cm). The other fragment has many small geopetals and borings of less than 0.5 cm.

70-114 cm

This interval contains three constituents: first a *M. annularis* complex fragment; second, a smaller fragment of another *M. annularis* complex and third, coral rubble. The first massive coral is one of the largest coral recovered with 29.5 cm long. It contains a layer of crustose red algae around (thickness: 6 mm) and some fragments of organisms found include those of *Halimeda sp.*, 10 serpulid tubes (0.1 to 2 mm), urchin spines and *H. rubrum*. Other features found were: 7 geopetals horizontally oriented, borings (0.5 cm to 5 cm), black and orange bands.

The second *M. annularis* complex fragment (4.5 cm long) and contains 7 serpulid tubes (0.5 mm to 1 mm diameter), borings (1 mm to 0.5 cm), and shows gray color. Mud was found in borings by using thin section analysis. Crustose red algae layer is found on top (thickness: 1 mm). Radiocarbon age in this sample resulted in 700 ± 25 yrs.

The coral rubble, is a group of 16 fragments: about three of these are acroporids, a bivalve shell and the rest of unknown origin. In general, these pieces are subangular and are covered by crustose red algae. Also, contain 7 serpulid tubes (< 1 mm to 1 mm diameter) and borings (< 1 mm to 1.5 cm).

114-136 cm

This interval is composed of four constituents: a fragment of *M. annularis* complex, coral rubble below, a fragment of *M. annularis* complex, followed by another fragment of a massive coral at the bottom. The first coral sample is 5.5 cm long and contain fragments of organisms such as articulate red algae in borings, 5 serpulid tubes (< 1mm to 1 mm diameter), *H. rubrum*, a layer of crustose red algae in the middle of the coral (thickness: 1mm) and a bivalve shell in burrow. Other features found: relatively many borings (1 mm to 1 cm) and shows gray color.

The coral rubble (below) is a group of 13 pieces of few identified as acroporids and mostly are of unknown origin. Many of these fragments are encrusted by crustose red algae (few pieces cemented) and contain about 18 serpulid tubes (0.5 mm to 1 mm diameter), sponge fragments, *H. rubrum* and borings (< 1 mm to 1 cm). These pieces are mostly angular to subangular.

A *M. annularis* complex fragment is found below (7.5 cm long). It contains crustose red algae in the middle of the coral growth (thickness: 1 mm), 9 serpulid tubes (0.5 mm to 1 mm diameter), borings (1 mm to 1 cm), *H. rubrum*, a mold of a bivalve shell and shows gray color (calcareous sediments).

The *M. annularis* complex fragment at the bottom (5.5 cm long), has a layer of crustose red algae in the middle of the coral growth (thickness: 2.5 mm), more than 20 serpulid tubes (0.5 mm to 2 mm diameter), *H. rubrum*, relatively high content of borings (1 mm to 1 cm) and is also gray colored at the edges. Acicular cement found by using thin section analysis.

REFERENCES

- Bak, R.P.M., (1994), *Sea urchin bioerosion on coral reefs: place in the carbonate budget and relevant variables*. Coral Reefs, 13, 99-103.
- Blanchon, P. and Perry, C.T., (2004), *Taphonomic differentiation on Acropora palmata facies in cores from Campeche Bank Reefs, Gulf of Mexico*. Sedimentology, 51, 53-57.
- Blanchon, P., Jones, B., Kalbfleish, W., (1997), Hurricane control on shelf-edge-reef architecture around Grand Cayman. Sedimentology 44, 479–506.
- Bowman, S., (1990), *Radiocarbon dating (Interpreting the past)*. University of California Press/British Museum.
- Bruggemann, J., van Kessel, A.M., van Rooij, J.M. and Breeman, A.M. (1996), *Bioerosion and sediment ingestion by the Caribbean parrotfish Scarus vetula and Sparisoma viride: implications of fish size, feeding mode and habitat use*. Marine Ecology Progress Series, 134, 59-71.
- Carricart-Ganivet, J.P., (2004), *Sea surface temperature and growth of the West Atlantic reef building coral Montastrea annularis*. Journal of Experimental Marine Biology and Ecology, 302, 249– 260.
- Chave, K. E., S. V. Smith, K. J. Roy., (1972), *Carbonate production by coral reefs*. Mar. Geol., 12, 123-140
- Darwin, C. R., (1842), *The structure and distribution of coral reefs. Being the first part of the geology of the voyage of the Beagle, under the command of Capt. Fitzroy, R.N. during the years 1832 to 1836*. London: Smith Elder and Co.
- Frydl, P., Stern, C.W., (1978), Rate of bioerosion by parrotfish in Barbados reef environments. Journal of Sedimentary Research, 48, 1149-1157.
- Flügel, E., (2004), *Microfacies of carbonate rocks: analysis, interpretation and application*. Springer-Verlag Berlin Heidelberg, p. 74-75.
- Goreau, T. F., and Hartman, W. D., (1963), *Boring sponges as controlling factors in the formation and maintenance of coral reefs*. In Soggneas, R. F. (Ed.), Mechanisms of Hard Tissue Destruction. Am. Assoc. Adv. Sci. Pub., 75, 25-54.
- Gygi, R.A., (1975), *Sparisoma viride (Bonnaterre), the stoplight parrotfish, a major sediment producer on coral reefs of Bermuda*. Eclog. Geol. Helv, 68, 327-359.
- Hallock, P. and Schlager, W., (1986), *Nutrient excess and the demise of coral reefs and carbonate platforms*. Palaios, 1, 389-398.

- Hubbard, D.K., Burke, R.B., Gill, I.P., Ramirez, W.R., Sherman, C., (2008), *Coral-reef Geology: Puerto Rico and the US Virgin Islands*. Coral Reefs of the USA, Springer Sc. and Buss Media B.V.
- Hubbard, D.K., (2008), *Depth and species related patterns of Holocene reef accretion in the Caribbean and western Atlantic: a critical assessment of existing models*. Spec. Publ. Int. Assoc. Sedimentol., 40, 1-18.
- Hubbard, D.K., Burke, R.B. and Gill, I.P., (1998), *Where's the reef: the role of framework in the Holocene*. Carbonates Evaporites, 13, 3-9.
- Hubbard, D.K., I. Gill, R. Burke, J. Morelock., (1997), *Holocene reef backstepping, southeastern Puerto Rico shelf*. Proc. 8 th Int. Coral Reef Symp., 2, 1779-1784.
- Hughes, T. P., Baird, A.H., Bellwood, D.R., Card, M., Connolly, S.R., Folke, C., Grosberg, R., Hoegh-Guldberg, O., Jackson, J.B.C., Kleypass, J., Lough, J.M., Marshall, P., Nystrom, M., Palumbi, S.R., Pandolfi, J.M., Rosen, B., Roughgarden, J. (2003), *Climate change, human impacts and the resilience of coral reefs*. Science, 301, 929-933.
- Humann, P., Deloach, N., (1992), *Reef Coral Identification: Florida, Caribbean, Bahamas*. New World Publications, Inc. Jacksonville, FL.
- Knowlton, N., Maté, J. L., Guzmán, H. M., Rowan, R., Jara, J., (1997), *Direct evidence of reproductive isolation among the three species of the Montastrea annularis complex in Central America (Panamá and Honduras)*. Marine Biology, 127: 705-711.
- Land, L.S., (1974), *Growth rate of a West Indian (Jamaican) Reef*. Proceedings of the Second International Cord Reef Symp 2.409-412.
- Lighty, R.G., MacIntyre, I.G., Stuckenrath, R., (1982), *Acropora palmata reef framework: a reliable indicator of sea level in the western Atlantic for the past 10,000 years*. Coral Reefs. 1, 125–130.
- Macintyre, I.G., (2007), *A History of Demise, Regeneration, and Survival of Coral Reefs in Response to Rising Seas of the Holocene Transgression: Examples from the Western Atlantic Region*. In R.B. Aronson ed. Geological Approaches to Coral Reef Ecology. New York. Springer-Verlag., 181-200.
- Moore, C.H. and Shedd, W.W., (1977), *Effective rates of sponge bioerosion as a function of carbonate production*. Proc 3rd Int Coral Reef Symp, 2, 499-505.
- Mora, C., (2008), *A clear human footprint in the coral reefs of the Caribbean*. Proc R Soc Lond B Biol Sci, 275, 767–773.
- Morelock, J., W. Ramírez, A. Bruckner, M. Carlo., (2001), *Status of coral reefs, southwest Puerto Rico*. Caribb. J. Sci. Special Publication No. 4.

- Neumann, A. C., (1966), *Observation on coastal erosion in Bermuda and measurement of the boring rate of the sponge Cliona lampa*. Limnol.Oceanogr. 11, 92-108.
- Pandolfi, J. M., Bradbury, R.H., Sala, E., Hughes, T.P., Bjorndal. K.A., Cooke, R.G., McArdle, D., McClenachan, L., Newman, M.J.H., Paredes, G., Warner, R.R. and Jackson, J.B.C., (2003), *Global trajectories of the long-term decline of coral reef ecosystems*. Science, 301, 955-958.
- Pandolfi, J.M., and Jackson, J.B., (1997) *The maintenance of diversity on coral reefs: examples from the fossil record*. Proceedings of the 8th International Coral Reef Symposium, Smithsonian Tropical Research Institute, Balboa, Republic of Panama, 397–404.
- Perry, C.T., Hepburn, L.J., (2008), *Syn-depositional alteration of coral reef framework through bioerosion, encrustation and cementation: Taphonomic signatures of reef accretion and reef depositional events*. Earth Science Reviews, 86, 106-144.
- Powers, M.C., (1953), *A new roundness scale of sedimentary particles*. Journal of Sedimentary Petrology, v. 23, p. 117-119.
- Rasser, M. W., Riegl, B., (2002), *Holocene coral reef rubble and its binding agents*. Coral Reefs, 21, 57-72.
- Reis, M.A.C., Leao, Z.M.A.N., (2000), *Bioerosion rate of the sponge Cliona celata (Grant 1826) from reefs in turbid waters, north Bahia, Brazil*. Proc. 9th Inte. Coral Reef symp., Bali, Indonesia.
- Ryan, K. E., J. P. Walsh, D. R. Corbett, A. Winter., (2008), *A record in recent change in terrestrial sedimentation in a coral reef environment, La Parguera, Puerto Rico: A response to coastal development?* Mar. Poll. Bull. 56, 1177-1183
- Scaps, P., Denis, V., (2008), *Can organisms associated with live scleractinean corals be used as indicators of coral reef status?* Atoll Research Bulletin, 566, 1-18.
- Shinn EA, Hudson JH, Halley RB, Lldz B (1977) Topographic control and accumulation rate of some Holocene coral reefs: South Florida and Dry Tortugas. Proc 3rd Int. Coral Reef Symp.: I-7
- Scoffin, T.P., (1987), *Introduction to Carbonate Sediments and Rocks*. P. 77. Blackwell, Glasgow.
- Scoffin, T.P., (1992), *Taphonomy of coral reefs: a review*. Coral Reefs, 11, 57-77.
- Steneck, R.S., Adey, W.H., (1976), *The role of environment in control of morphology in Lithophyllum congestum, a Caribbean algal ridge builder*: Botanica Marina, 19, 197–215.

- Szmant, A. M., Weil, E., Miller, M.W. and Colón, D.E., (1997), *Hybridization within the species complex of the scleractinian coral *Montastraea annularis**. *Marine Biology*, 129, 561-572.
- Tucker, M. E., V. P. Wright, (1990), Carbonate sediments and limestones: constituents. In *Carbonate sedimentology*, ed. Wright, P., 1-27. Oxford, UK: Blackwell Publishing.
- Van Veghel, M.L.J., Bak, R.P.M., (1993), *Intraspecific variation of dominant Caribbean reef building coral, *Montastrea annularis*: genetic, behavioral and morphometric aspects*. *Mar. Ecol. Prog. Ser.*, 92, 255-265.
- Vecsei, A., (2004), *A new estimate of global reefal carbonate production including the fore-reefs*. *Global and Planetary Change*, 43, 1 –18.
- Wai, T. and Williams, G., (2005), *The relative importance of herbivore-induced effects on productivity of crustose coralline algae: Sea urchin grazing and nitrogen excretion*. *Journal of Experimental Marine Biology and Ecology*, 324, 141– 156.